C.P. No. 381
(19,836)
A.R.C. Technical Report

C.P. No. 381
(19,836)
A.R.C. Technical Report

MINISTRY OF SUPPLY

AERONAUTICAL RESEARCH COUNCIL

CURRENT PAPERS

Measurements of the Effect of Surface Cooling on Boundary Layer Transition on a 15° Cone

Part 1. Tests at $M = 2$ and 3 in an 8 in. x 9 in. Wind Tunnel at R.A.E. / Bedford

By

A. C. Browning, J. F. W. Crane and R. J. Monaghan

LONDON: HER MAJESTY'S STATIONERY OFFICE

1958

SIX SHILLINGS NET

C.P. No. 381

U.D.C. No. 533.6.011.5 : 533.6.011.6 : 532.526.3 : 533.691.18

Technical Note No. Aero.2527

September, 1957

ROYAL AIRCRAFT ESTABLISHMENT

Measurements of the effect of surface cooling on boundary layer transition on a 15° cone.

Part I. Tests at M = 2 and 3 in an 8 in. x 9 in. wind tunnel at R.A.E./Bedford

by

A. C. Browning, J. F. W. Crane
and
R. J. Monaghan

SUMMARY

Tests on a steel cone of 15° included angle, cooled internally by the circulation of cold alcohol, gave the results that when the ratio (surface temperature ahead of transition)/(surface temperature for zero heat transfer) was reduced from 1.0 to 0.88, the transition Reynolds number at zero incidence was increased by a factor of about 1.8 for a local Mach number (M_1) of 1.86 and by a factor of 1.24 - 1.43 for M_1 = 2.81. The spread in the latter factor arose from alternative estimates of transition Reynolds number under zero heat transfer conditions, since at M_1 = 2.81 this Reynolds number was dependent on stagnation pressure. (This effect might be explained by the presence of an adverse pressure gradient over the rear of the cone at this Mach number.)

Simultaneous records of transition position on the top and bottom generators of the cone were obtained in all cases, using the shadowgraph technique.

When the cone was set at an incidence of 2°, transition on the windward generator moved aft with cooling at about the same rate as was found in the zero incidence tests (at each Mach number). However, little, if any, movement could be discerned on the leeward generator.

Further tests at M = 3, 4 and 4.5 will be made at R.A.E./Farnborough.

LIST OF CONTENTS

LIST OF APPENDICES

TABLE

LIST OF ILLUSTRATIONS

1 Introduction

It is by now a well known theoretical result that withdrawal of heat from a laminar boundary layer should increase its stability to small two-dimensional disturbances. Indeed if the external flow is supersonic and its Mach number is less than about ten, the theory presented by Lees[1] (an extension of the Tollmien-Schlichting theory of incompressible flow) and further developed by Van Driest[2], indicated that if the cooling rate were sufficient, then the laminar boundary layer could be made completely stable. The amount of cooling (expressed in terms of reduction of surface temperature below that for zero convective heat transfer) required to obtain this ideal state of affairs would be at a minimum around M = 2, but would then increase with increasing Mach number until for Mach numbers around ten it would be impossible to achieve complete stability.

More recently, Dunn and Lin[3] have shown that for Mach numbers greater than two, three-dimensional disturbances may play a leading role in determining the stability of the laminar boundary layer and complete stability by cooling cannot be achieved with respect to all three-dimensional disturbances. However, surface cooling may still be an effective means of delaying the onset of instability.

These theories give "minimum critical Reynolds numbers" below which all small disturbances are damped out. As yet they cannot be related to the transition Reynolds numbers obtained in practice and in addition the latter may be dominated by effects such as roughness, pressure gradients*, shock waves and, in wind tunnel tests, tunnel turbulence. However, if the turbulence level is low, transition on a smooth body clear of extraneous shock waves might be expected to vary with cooling rate and Mach number in a manner similar to that calculated for the minimum critical Reynolds number. This indeed was the case with the correlation of experimental results in Ref.5, which gave fourfold and tenfold increases in transition Reynolds number when the ratio of surface temperature to zero heat transfer temperature was reduced from unity to 0.80 and 0.68 respectively. However, the local Mach numbers involved were mainly in the range $1.5 < M < 2.5$, and this is the region where theory predicts that cooling should be most effective. The query then arises as to how these results might be modified if the local Mach number were higher and this was the reason for the present series of tests.

The intention is to measure the effect of surface cooling on the transition Reynolds number on a cone over a Mach number range from 2 up to about 4.5. A cone was chosen for the test body since at supersonic speeds there is zero pressure gradient along its length (assuming uniform flow conditions in the working section of the wind tunnel) and, when mounted in the centre of a wind tunnel, it is free from interference with tunnel wall boundary layers, unlike a flat plate spanning the working section. The dimensions were chosen to give Reynolds numbers as large as possible when tested at the higher Mach numbers in the No.5 Supersonic Tunnel at R.A.E./Farnborough. This meant that tests could not be made at Mach numbers less than three, because of tunnel blockage, so, additional tests were scheduled for the 8 in. × 9 in. Supersonic Tunnel in the High Speed Laboratory of R.A.E./Bedford at M = 3 (for comparison with the No.5 Tunnel) and at M = 2 (for comparison with the correlation of Ref.5).

The tests at R.A.E./Bedford were made first and the results are given in the present note. Tests are now being made at M = 3, 4 and 4.5 in the No.5 Tunnel at R.A.E./Farnborough and the results will be given in subsequent notes.

---

* A theoretical treatment of the two-dimensional problem including pressure gradients may be found in Ref.4.

Since earlier tests had shown that small amounts of incidence could have a very marked effect on transition position under zero heat transfer conditions[6], the cooling tests are being made at incidences of 0° and $+2^{\circ}$. All the transition results in the present note were obtained from shadowgraph pictures and correspond roughly to the end of the transition "region". Another note is being issued which compares transition estimates given by shadow, schlieren, pitot, sublimation and oil-flow techniques[7], which were all tried out before the main test series began.

Finally, the authors would like to acknowledge the willing co-operation and assistance afforded to them by members of the staff of R.A.E./Bedford, both before and during the tests, which extended over the period November 1955 to April 1956.

2 Apparatus and techniques

2.1 The No.1 Supersonic Tunnel, High Speed Laboratory, R.A.E./Bedford

This is a new facility and is a return flow wind tunnel with a working section 8 inches high by 9 inches wide. It is powered by a B.T.H. four stage centrifugal compressor, electrically driven, with Ward Leonard speed control. A small auxiliary compressor is provided for pressurising or evacuating the circuit. Liners for M = 2 and M = 3 were available and the operating conditions appropriate to the tests described in this note are tabulated below

M_{∞}	M_1	Maximum Stagnation Pressure (Atmospheres)	Stagnation Temperature ($^{\circ}C$)	Maximum Local Reynolds Number Per Inch $\times 10^{-6}$
1.97	1.86	3	38	0.918
3.01	2.81	4	40	0.755

2.11 Uniformity of flow in the working section

Before commencing each test series a calibration of the flow in the working section was made with a pitot rake. With M = 3 liners and for a stagnation pressure of two atmospheres, the calibration revealed a maximum variation of ± 0.75 per cent from a mean Mach number of 3.01. Subsequent runs with a 15° stainless steel cone model sprayed with azobenzene (sublimation indicator of transition) showed up disturbances which could be traced back to the window joints A and B in Fig.3. An attempt was made to reduce the wall discontinuity at B by filling with Picien wax, but this made little difference to the shock strength. At this Mach number, the most forward point on the cone at which the disturbances showed up was two inches from the base, but when transition occurred in this region, the shape of the transition front, indicated by azo-benzene, did not appear to be affected by them*.

The calibration with the M = 2 liners was carried out after the M = 3 test series and showed a mean Mach number of 1.97 with a maximum variation of ± 1.15 per cent. A cone sprayed with azo-benzene showed up disturbances coming in from the side walls and reflecting at a most forward point of three inches from the tip. Once again no affect on the shape of the transition front was observed.

---

* The disturbances mentioned above were observed when the flow was laminar over the whole length of the cone.

The final distributions of Mach number along the 15° pressure cone are given in Fig.7 and discussed in Section 3.1.

2.12 The settling chamber, screens and filters

The approach to the working section consists of a 20 foot length of steel pipe of $2\frac{1}{2}$ feet internal diameter, followed by a settling chamber of maximum cross-section 43.6 inches square and of overall length 16 feet. The mean air velocities in the 43.6 inch square section were 14.5 ft/sec (T_{H1} = 311°K) for M = 2, and 5.8 ft/sec (T_{H1} = 314°K) for M = 3.

For the tests at M = 3 the two wire gauze (60 mesh) turbulence reducing screens, spaced 2 feet apart in the settling chamber, were supplemented by four layers of buttermuslin fitted to the upstream gauze. The buttermuslin was added to arrest alumina dust (from the dryers) which had contaminated the circuit and had eroded model surfaces and interfered with optical observation of the airflow. The buttermuslin was cleaned quite frequently and was sprayed with oil to facilitate dust adhesion.

For the tests at M = 2, the buttermuslin filter was replaced by a filter consisting of 1/16 inch pressed woollen felt (Specification No. D.T.D.590) on a wire gauze (32 mesh and No.32 Imperial Standard wire gauge). This proved to be a far superior dust filter and needed considerably less attention. The properties of this type of filter are described in another note[8].

2.13 Air drying and temperature control

The air is dried on entering the tunnel circuit by filtering through activated alumina granules and is maintained in a dry condition by continuous by-passing of a fraction of the flow through the circuit dryer. The amount by-passed is controlled by a valve, the opening of which can be calibrated to maintain the required humidity.

A Cassella dew-point meter, tapped onto the high pressure end of the tunnel and exhausting to atmosphere, was used to check the humidity control.

For the first series of tests at M = 3, the dew-point measurements were made fairly frequently and showed a reasonably constant humidity level. The maximum value of absolute humidity measured was 3×10^{-4} lb/lb, which would have an effect of increasing the zero heat transfer temperature on a model by less than 1°C above that obtained with perfectly dry air.

For the second test series, at M = 2, dew-points were measured in the first two tests and the by-pass valve was adjusted to maintain the level of absolute humidity between 1.5 to 3×10^{-4} lb/lb. The effect on zero heat transfer temperature would be similar to that in the M = 3 tests. No further measurement of the dew-point was made, experience having proved the efficiency of the dryers and the reliability of the valve setting for humidity control.

The temperature of the air was controlled by regulation of the water flow through the air cooler in the tunnel circuit, and temperature limitations on the compressor set an upper limit to the stagnation temperature attainable.

2.14 Optical system

The optical system, shown in Figs.1 and 2, is a standard two-mirror schlieren system having spherical mirrors of twelve inches diameter and ten feet focal length.

2.2 Models

2.21 15° Static pressure cone (copper)

This model is shown in Fig.3, loosely mounted in the tunnel. It is a sharply pointed 15° cone nine inches long. The frustrum is of copper with a butt-welded seam, and has a nominal wall thickness of 0.050 inches. The tip is separately machined from copper bar and soldered into position. Eighteen $\frac{1}{2}$ mm pressure holes are spaced mainly along two opposite generators of the cone and are formed by 1 mm outside diameter copper nickel tubes flush soldered into the skin. These tubes are passed through the steel base, which is attached by four screws to the cone shell, and are then connected by P.V.C. tubes to a manometer bank. A No.4 Morse taper on the base provides the attachment to the model mounting. Some repairs with solder are visible in the photograph.

2.22 15° Heat transfer cone (mild steel)

Details of this model are given in Fig.4. The cone is 9 inches in length, excluding 'araldite' resin sealing at the base, and is attached to an integral base plug and sting. Mild steel was chosen for the cone because of its comparative ease of fabrication and machining. The cone frustrum was machined from bar and it has a wall thickness of 1/10 inch. The conical nose piece was separately machined and was attached to the frustrum with soft solder.

The average surface roughness, measured by Talysurf profilograph, was 10 micro-inches r.m.s. The tip radius, deduced from an enlarged shadowgraph picture (Fig.5b), was 0.0015 inches, giving maximum Reynolds numbers based on tip radius and undisturbed flow conditions of 1370 at $M_\infty = 1.97$ and $p_o = 3$ atmospheres, and 1100 at $M_\infty = 3.01$ and $p_o = 4$ atmospheres.

Thermocouple junctions (steel/constantan, using the skin of the cone and an attached mild steel wire as a common return) are spaced mainly along the upper and lower generators of the cone as indicated in Fig.4. Details of the installation and calibration of these thermocouple junctions are given in Appendix I, and some discussion of the requirements regarding surface condition in their neighbourhood (Fig.5a) is given in Appendix III. Two further thermocouple junctions are positioned centrally in the coolant inlet and outlet passages in the cone sting.

The cone was cooled by an internal circulation of cold alcohol using the cooling system shown in the schematic diagram of Fig.6 and described fully in Appendix II. This cooling system proved to be very successful in maintaining steady surface temperatures.

The sting mounting was similar to that used for the 15° static pressure cone.

2.23 15° Stainless steel cone (uninstrumented)

This model is a sharply pointed cone, 9 inches in length made from stainless steel bar. No instrumentation is fitted, the model being used mainly for independent checks on zero heat transfer transition results. The surface finish was of the order of 10 micro-inches r.m.s.

The results for transition at zero heat transfer obtained with this cone, by both optical and chemical indicator methods, agreed with the results obtained with the mild steel cone using the same methods under the same conditions.

2.3 Model mounting and setting

From Fig.3 it may be seen that the models were mounted on an extremely rigid wedge beam support, positioned vertically on the centre-line of the tunnel at the rear end of the working section. The beam is a machined forging in steel with drillings for coolant flow and for thermo-couple wires. Fabricated steel boxes, mounted flush with the liners and bolted to the tunnel shell, provide anchorage for the beam. Yaw and incidence settings are obtained on adjustable plates and final locking is by large nuts bearing on spherically seated washers.

Incidence and yaw of each model was measured relative to the bottom liner and starboard sidewall. This was accomplished by means of a vernier scale bevel protractor and engineers' blocks, using the appropriate cone generator as a reference line. An accuracy in angular measurement of ±2 minutes was obtained. True zero was taken as the tunnel centre line.

2.4 Measuring Techniques

2.41 Test procedure

(a) Zero heat transfer

For this condition the cone was free of coolant. Supersonic flow over the model was established at a low pressure in approximately 3 to 5 minutes from the start of the main compressor. The auxiliary compressor was then used to increase the total mass of air in the circuit and thus raise the stagnation pressure to the desired value. A warming up process then ensued until the required steady stagnation temperature was reached. This occupied a time of between 10 and 30 minutes according to the initial temperature of the pipework and the selected mass flow of air.

With the stagnation pressure held to within ±0.2" Hg and the stagnation temperature controlled to within $\pm\frac{1}{4}^{\circ}$C, a plot of the cone temperature distribution was made and shadowgraph pictures were taken.

(b) Cooling tests

The technique for the cooling tests was similar to that for the zero heat transfer tests except for the additional requirement of a steady flow of coolant at constant temperature into the model.

Thermocouple 2.6 T (2.6 inches slant length from the tip, on the top generator) was used as a control in these tests, and complete surveys of the lengthwise temperature distribution were made at intervals. Tests were made with the coolant flowing from base to tip and vice versa.

2.42 Measurement of stagnation pressure

The stagnation pressure was taken from a pitot mounted at the centre of the settling chamber and was measured by a Midwood automatic self-balancing capsule manometer[9]. This particular manometer had a range of 0 to 4 atmospheres absolute and a measuring accuracy of ±0.01 inches of mercury.

2.43 Measurement of stagnation temperature

The stagnation temperature was measured by an Elliott electrical resistance thermometer having its sensitive element positioned at the above pitot in the settling chamber. The thermometer had a large horizontal scale covering a range of 0 to 50°C and had a measuring accuracy of $\pm\frac{1}{4}^{\circ}$C.

2.44 Measurement of static pressures on the 15° pressure cone

The static pressure distribution along the pressure cone was measured on a bank of mercury manometers which had a backing screen graduated in tenths of an inch. The reference pressure was ambient atmospheric. There were no cocks in the system.

2.45 Temperature measurement on the heat transfer cone

The layout of the temperature measuring equipment is shown in Fig.1. Thermocouple e.m.f. values were measured on a Tinsley constant resistance potentiometer and mirror galvanometer, using a near null system with a least count of one microvolt (equivalent to $^1/_{50}$°C for the steel/constantan couple). A thermostatically controlled, electrically heated Sunvic "cold junction" thermostat was maintained at a constant temperature of +41°C as measured by a calibrated mercury thermometer.

2.46 Measurement of the transition position

The shadowgraph method was chosen to record transition after a comparative study had been made of a number of methods[7]. The advantages of this method are its speed and ease of operation, its independence of model surface temperature, and its ability to record transition on both generators simultaneously. The latter is a most important feature bearing in mind the sensitivity of transition position to small incidence changes on a body of revolution in supersonic flow.

The boundary layers on the cone were very thin, but examination of a shadowgraph picture revealed an image due to the refraction of light through the turbulent boundary layer superimposed on and above the diffraction lines at the cone boundary. The boundary of this image approximates to the theoretical turbulent boundary layer thickness, and by viewing it obliquely to increase its gradient, the point of intersection with the main diffraction band at the cone boundary may be marked to within $\pm\frac{1}{8}$ inch*. The transition position interpreted in this manner corresponds to the end of the transition region[7].

Circumferential similarity of transition position was checked both by oil flow and chemical sublimation techniques.

The shadowgraph pictures were taken with parallel light rays from a mercury vapour lamp passing through a measuring grid onto hard bromide photographic paper positioned close to the tunnel, and long exposure times of between 20 and 30 seconds were used.

3 Results and discussion of tests at zero incidence

In these tests the cones were set at zero incidence relative to the centre line of the tunnel. The subsequent transition results indicate that this may not have been true zero relative to the airstream, but the difference was probably very small (see Section 3.3 below).

3.1 Mach number distributions along the top and bottom generators of the 15° copper cone

The static pressures measured on the 15° copper cone were combined with the stagnation pressure, (a correction for the small loss through the tip shock would be within the experimental accuracy) to give the Mach number

---

* This corresponds approximately to $\pm 0.1 \times 10^6$ in transition Reynolds number at the highest stagnation pressures used (cf. the table of operating conditions in Section 2.1).

distributions show in Fig.7. These distributions were obtained mainly to give a check on the performance of the tunnel (which was a new facility) and some of the scatter in the results may be due to the surface condition of the copper cone in the neighbourhood of the static pressure orifices, which was not ideal.

Fig.7a shows the results for a nominal tunnel Mach number (M_∞) of 2.0 and a stagnation pressure (p_o) of 3 atmospheres (the highest available pressure at that Mach number). There are appreciable variations in local Mach number (M_1) over the first 4 inches of the cone which might be related to the tunnel disturbances mentioned in Section 2.11, but aft of that station the flow becomes sensibly uniform, with good agreement between results from the top and bottom generators. Transition on the steel cone always occurred aft of 4 inches from the tip, so, from Fig.7a, the local Mach number was taken to be 1.86, corresponding to a tunnel Mach number of 1.97, which is $1\frac{1}{2}$ per cent. below the design value.

Fig.7b shows the results for nominal $M_\infty = 3.0$ and $p_o = 4$ atmospheres. In this case the distribution is fairly uniform over the first 6 to 7 inches of the cone, but there is evidence of an adverse pressure gradient over the last 2 to 3 inches (which also may be related to the tunnel disturbances mentioned in Section 2.11). Transition generally occurred downstream of x = 5 inches and therefore may be affected by this pressure gradient in some cases. The local Mach number was taken to be $M_1 = 2.81$, corresponding to a tunnel Mach number of 3.01, which is $\frac{1}{3}$ per cent. above the design value.

Tests at lower stagnation pressures showed no significant effect of stagnation pressure on the distributions at either Mach number.

3.2 Surface temperature distributions along the top and bottom generators of the 15° mild steel cone

This was the cone used in the transition tests and Figs.8 and 9 give representative surface temperature distributions obtained during these tests. Short vertical lines through the curves show the corresponding transition positions indicated by the shadowgraph. (The full lines are for the top generator and the broken lines are for the bottom generator.)

Fig.8 is for $M_\infty = 1.97$ and $p_o = 3$ atmospheres. Fig.9 is for $M_\infty = 3.01$ and $p_o = 4$ atmospheres.

At one stage it had been hoped that transition could be deduced from the surface temperature distributions. This is feasible under zero heat transfer conditions, as evidenced by the shape of the topmost curves in Figs.8 and 9 and their comparison with the temperatures which would be expected with temperature recovery factors (r) of 0.85 (laminar) and 0.88 (turbulent). Note that the shadowgraph indications are near to the beginning of the fully turbulent region.

However, the task becomes much more difficult when the cone is cooled, since the surface temperatures then become dependent upon the internal as well as upon the external distributions of heat transfer coefficients. This is illustrated by comparing the results obtained when the coolant was flowing from the base to the tip of the cone (Fig.8a, 9a) with those obtained when the coolant was flowing in the opposite direction (Figs.8b, 9b). Additional thermocouple stations would be needed before a quantitative analysis could be made of these curves.

In the later analysis of the transition results (Section 3.3), these temperature distributions had to be used to give values of surface temperature appropriate to the laminar boundary layer before transition. Two possibilities were available. The first was to take the lowest temperature

reading (at x = $2\frac{1}{2}$ inches) to be representative of the laminar layer. The second was to choose the temperature at the inflexion point on the "plateau" before the steep rise on the curves. The latter would seem to be the better choice, but, as Figs.8 and 9 show, it cannot be chosen so accurately, mainly because the limited number of thermocouple stations left room for an amount of imagination when trying to draw in faired curves. At this stage it may be worth noting that an error of 3°C in surface temperature would cause a change of 0.01 in the surface temperature ratios used later (Section 3.3 and Figs.11 and 12).

A further point is that the stability theories for the laminar boundary layer assume that the surface temperature is uniform. In accelerating flight without internal cooling, the surface temperature would decrease with increasing distance from the nose, as long as the boundary layer remained laminar. On the other hand, the present tunnel results show an increasing surface temperature with increasing distance from the nose until the layer is fully turbulent, (although it is probable that the tip temperature is close to zero heat transfer at all times, so that there would be a decrease in surface temperature over the first inch or so of the cone).

Temperature gradients may have their effect on the stability of the laminar boundary layer, so from the above considerations it seemed advisable to concentrate on results obtained with the coolant flowing from the base to the tip of the cone since this gave more uniform temperature distributions (Figs.8a and 9a, by comparison with Figs.8b and 9b).

3.3 Transition results from shadowgraph pictures

3.31 Zero heat transfer conditions

Figs.10a and 10b give the transition Reynolds numbers, (based on local flow conditions, R_{T_o}) on the top and bottom generators of the cone under zero heat transfer conditions at M_∞ = 1.97 and 3.01, over ranges of stagnation pressure. In both cases transition occurred later on the top than on the bottom generator, which might indicate[6] that the cone was at a small negative angle of incidence to the airstream. However, the subsequent cooling tests showed a good measure of agreement between results from the top and bottom generators (by sharp contrast to the tests at $\alpha = +2^\circ$ in Section 4), so no corrections were made. In any case, differential transition might be caused by the flow non-uniformities exhibited in Fig.7.

The more notable feature in Fig.10 is that while the transition Reynolds number at M_∞ = 1.97 (Fig.10a) remains sensibly constant while p_o increases from 2 to 3 atmospheres, at M_∞ = 3.01 it increases from 3 to 4 million while p_o increases from 2 to 4 atmospheres. This remains an unexplained anomaly. Possibilities are (1) an effect of tip thickness and (2) an effect of pressure gradients.

Concerning the first possibility, the Reynolds number based on tip radius and undisturbed flow conditions would have been about 1370 at M_∞ = 1.97 and p_o = 3 atmospheres and about 1100 at M_∞ = 3.01 and p_o = 4 atmospheres, so no significant difference between the two sets of results might be expected from this cause. In any case, with corresponding transition Reynolds numbers of 3 to 4 million, the outer edge of the boundary layer should be well clear of the tip influence region discussed by Moeckel in Ref.10. (It is intended to make some transition tests on cones with blunt tips, which may help to clarify this point.)

Concerning the second possibility, the scales at the tops of Figs.10a and 10b show approximately where transition occurred on the top generator of

the cone*. At $M_\infty = 1.97$, (Fig.10a) the range is roughly from 5 to 7 inches from the tip, which is in a fairly uniform flow region according to Fig.7a. On the other hand, at $M_\infty = 3.01$ (Fig.10b) the range is from 5.5 to 8 inches from the tip and Fig.7b shows that the region downstream of $6\frac{1}{2}$ inches was under the influence of adverse pressure gradients. These pressure gradients might explain the drop in transition Reynolds number as the stagnation pressure was reduced**.

Finally, the transition Reynolds numbers at $M_\infty = 3.01$ under zero heat transfer conditions are fairly good average values by comparison with results obtained elsewhere on cones[5], but those at $M_\infty = 1.97$ are somewhat on the low side.

3.32 Effect of cooling

The cooling tests were made at constant stagnation pressure. At each Mach number the highest available stagnation pressure was used in order to ensure that transition always occurred ahead of the base of the cone. The results are given in Table I and are plotted in Figs.11 and 12.

The cone was not disturbed in between the tests of each set, which include a range of cooling conditions and a check test at zero heat transfer. The transition Reynolds number from the latter was taken to be the datum value for the set under consideration (except where noted in Table I, or in the alternative analysis of Section 3.322) and it can be seen that there was some variation in this datum between sets. The values may differ also from those obtained in the earlier tests at zero heat transfer and the reasons for these variations are probably small differences in cone setting in the tunnel, allied with small variations in surface condition.

3.321 $M_\infty = 1.97$, ($M_1 = 1.86$) and $p_o = 3$ atmospheres

These results are plotted in Fig.11 for the top and bottom generators of the cone and for the two directions of coolant flow. The plots are of transition Reynolds number based on local flow conditions ($M_1 = 1.86$) against the ratio of actual surface temperature (T_w) to estimated surface temperature for zero heat transfer with a laminar boundary layer (T_{wo}), assuming a recovery factor of 0.85 (cf. Fig.8).

As discussed in Section 3.2, the surface temperature was by no means uniform and there was some difficulty in choosing a value of T_w representative of the laminar boundary layer.

The first choice was to take the value of T_w at $x = 2\frac{1}{2}$ inches on the top generator, and this gives the values in Fig.11a. It is notable here that the results from the two coolant flow directions diverge at the lower values of T_w/T_{wo}. Reference to Fig.8b shows that when low surface temperatures were being sought with the coolant flowing from the tip to the base, the temperature at $x = 2\frac{1}{2}$ inches could be much lower than the temperatures obtained over the remainder of the cone. For this reason the results for coolant flow from base to tip seem more reliable, but even then the values of T_w/T_{wo} are probably on the low side (cf. Fig.8a).

---

* Also see Fig.13a which gives direct plot of R_T against x_T for $M_\infty = 3.01$.

** Preliminary results of the subsequent tests at R.A.E./Farnborough support this thesis, in that very little movement in transition Reynolds number with stagnation pressure is being obtained at $M_\infty = 3.1$.

The second choice was to take the temperature at the inflexion point before the steep rise of curves such as in Fig.8 to be representative of the temperature of the laminar boundary layer before transition. This seems more logical and the corrections were mainly small in the case of coolant flow from base to tip (3°C corresponds to about 0.01 in T_w/T_{wo}). Larger corrections were necessary in some instances when the coolant was flowing from tip to base and there is obviously a margin of error in both cases, as mentioned in Section 3.2.

The result of making this second choice is shown in Fig.11b. The results from the two coolant flow directions are more consistent than in Fig.11a and, as might be expected, R_T increases more rapidly with decreasing T_w/T_{wo}.

To eliminate the effect of variations of transition Reynolds number under zero heat transfer conditions (R_{T_o}), the results (taking T_w at the inflexion point) are re-plotted in Fig.11c as the ratio R_T/R_{T_o} against T_w/T_{wo}, taking R_{T_o} from the faired curves of Fig.11b. A mean curve has been drawn through the collected results and this lies somewhat below the mean correlation curve of Ref.5.

However in view of the difficulty in determining representative values of T_w and since the flow over the first 4 inches of the cone may have been rather non-uniform (cf. the flow distributions for the copper cone in Fig.7a), the discrepancy between the two curves is not considered to be significant.

3.322 $M_\infty = 3.01$ ($M_1 = 2.81$) and $p_o = 4$ atmospheres

These results are plotted in Fig.12 and all the plotting details are the same as in Fig.11.

Once again, taking T_w at the inflexion point improves the consistency of the results obtained with the two coolant flow directions (Fig.12b compared with Fig.12a).

The remarkable (and disturbing) feature is that the movement of transition Reynolds number with cooling is very much less than was found at $M_\infty = 1.97$ (Fig.12c). For example, when $T_w/T_{wo} = 0.9$, R_T/R_{T_o} is only about 1.2 at $M_\infty = 3.01$ ($M_1 = 2.81$) compared with about 1.6 at $M_\infty = 1.97$ ($M_1 = 1.86$).

Support for a decrease in cooling effectiveness is given by the mean curve derived from Jack and Diaconis' results for a $9\frac{1}{2}^\circ$ cone in an $M_\infty = 3.12$ airstream[11], (giving $M_1 = 3.0$). (The model used by Jack and Diaconis was a cone-cylinder, but in deriving the mean curve in Fig.12c, only the results for transition on the cone were used.) This mean curve is seen to agree well with the present results for a 15° cone and $M_1 = 2.81$.

However, if there is such a marked decrease in cooling effectiveness when M_1 is increased from 1.86 to 2.81 (or 3.0), then one might reasonably expect the present results at $M_1 = 2.81$ to lie above those obtained by Jack and Diaconis at $M_1 = 3.0$. The reason why they do not may be because there was an adverse pressure gradient over the rear of the cone in the present tests (Fig.7b). Thus, transition under zero heat transfer conditions occurred between $5\frac{1}{2}$ and 6 inches from the tip of the cone and moved back to $7\frac{1}{2}$ to 8 inches when the cone was cooled to $T_w/T_{wo} = 0.86$. Hence the cooled results would enter the region of adverse pressure gradient shown in Fig.7b and this could keep the transition Reynolds numbers low.

We have suggested already that this adverse pressure gradient may be a causal factor in the variation of transition Reynolds number with stagnation pressure, found under zero heat transfer conditions at $M_1 = 2.81$ (Section 3.2 and Fig.10b). This suggests an alternative analysis of the cooling results, if we assume that transition Reynolds number is a function of distance along the cone (i.e. of the position in a flow field which does not vary with stagnation pressure: note the last sentence of Section 3.1), as well as of the value of T_w/T_{wo}.

Applying this suggestion, Fig.13a shows the transition Reynolds numbers obtained under zero heat transfer conditions with varying stagnation pressure (curve B) and the transition Reynolds numbers obtained in the cooling tests at constant stagnation pressure (curve A), both plotted against the distance of the transition point from the tip (x_T). (For clarity, only the results for the top generator and with coolant flowing from base to tip, as shown.) As already mentioned at the head of Section 3.32, the transition Reynolds numbers under zero heat transfer conditions show some scatter, so a further curve (C) was added, which is parallel to curve B and goes through the zero heat transfer value on curve A.

It was then assumed that curve C would give the zero heat transfer values of transition Reynolds number corresponding to the cooled results on curve A, e.g. if with a certain degree of cooling, transition occurs 7 inches from the tip then the corresponding zero heat transfer transition Reynolds number is about 3.8 million, instead of the 4.3 million assumed in the earlier analysis.

This may seem to be an artificial procedure, but in fact it is that which would be used if transition was being determined from a fixed pitot, say 7 inches from the tip, in which case when the cone was cooled, the stagnation pressure would be altered until transition occurred at the pitot and the corresponding Reynolds number would be taken as the appropriate value.

Combining curves A and C gives values of R_T/R_{T_o} which are plotted against T_w/T_{wo} in Fig.13b (combined symbols) and the mean curve (full line) is considerably above that deduced with constant R_{T_o} in the earlier analysis.

At this stage the only conclusion which may be drawn is that, without pressure gradients, the variation of R_T/R_{T_o} with T_w/T_{wo} at $M_1 = 2.81$ might lie within the region enclosed by the two curves labelled "$M_1 = 2.81$" in Fig.13b. The check tests in the No.5 tunnel at R.A.E./Farnborough may help to clarify this point.

The mean curve for $M_1 = 1.86$ would not be altered by a similar alternative analysis, since the transition Reynolds number under zero heat transfer conditions did not vary with stagnation pressure (Fig.10a).

So, in summary, it can be said that for $T_w/T_{wo} = 0.9$, while $R_T/R_{T_o} = 1.87$ from the mean curve of Ref.5 for $1.5 < M < 2.5$, the present tests give values of 1.6 at $M_1 = 1.86$ and 1.19 to 1.32 at $M_1 = 2.81$*.

---

* The comparison with Ref.5 in this instance might better be made in values of T_w/T_{wo} for the same R_T/R_{T_o}, since the curves are steep. Thus $R_T/R_{T_o} = 1.87$ corresponds to $T_w/T_{wo} = 0.90$ from the mean curve of Ref.5 and 0.875 from the present tests at $M_1 = 1.86$. The corresponding extrapolated values at $M_1 = 2.81$ would be ? - 0.815, and at $M_1 = 3.0$ (Jack and Diaconis) 0.6 - 0.65.

The mean curve derived from Jack and Diaconis[11] gives $R_T/R_{T_o} = 1.19$ when $T_w/T_{wo} = 0.9$ at $M_1 = 3.0$. Thus there is evidence that the effectiveness of cooling in delaying transition decreases with increasing Mach number above 2.

By way of comparison with flight conditions, it may be noted that for a 15° cone flying in the stratosphere at $M_\infty = 1.97$ and 3.01, the laminar values of T_{wo} would be 360°K and 545°K respectively. The present results extend down to $T_w/T_{wo} \simeq 0.85$, which would correspond to surface temperatures of 306°K (33°C) and 463°K (190°C) respectively. The latter value is roughly the (laminar) equilibrium temperature at the station corresponding to R_x = 10 million in flight at $M_\infty = 3$ at 50,000 ft, with a surface emissivity of 0.9.

4 Results and discussion of tests at an incidence of +2°

In these tests the steel cone was set at an incidence (α) of +2° relative to the centre line of the tunnel. This would introduce a circumferential variation of Mach number around the cone surface (in inviscid flow) but the condition of zero pressure gradient should still be satisfied along the generators. The test results of Ref.6 showed that theoretical estimates of the pressure field and of the laminar boundary layer development on cones at small incidence should be valid under the test conditions. Also, under zero heat transfer conditions, there should be a marked difference in transition position between the top (leeward) and bottom (windward) generators[6].

The variations in local Mach number and Reynolds number introduced on a 15° cone by changing the incidence from 0° to 2° would be small and the analysis of the present test results was based on values derived for zero incidence. This gives a direct comparison with the results of Section 3 and, in addition, small variations in incidence or yaw in a flight case would be largely accidental and it is convenient to have the answers expressed in terms of conditions appropriate to zero incidence.

Coolant flow was from base to tip during these tests.

4.1 Surface temperature distributions

Sample temperature distributions along the top and bottom generators of the 15° steel cone at +2° incidence are given in Fig.14. Fig.14a gives the results for $M_\infty = 1.97$ and p_o = 3 atmospheres. Fig.14b is for $M_\infty = 3.01$ and p_o = 4 atmospheres.

The solid curves refer to the top (leeward) generator, the broken curves to the bottom (windward) generator and the short vertical lines show where transition was indicated by the shadowgraph pictures.

As the cooling rate is increased there is an increasing divergence between the temperature distributions on the top and bottom generators. This is in accord with axial asymmetry in boundary layer growth (and hence in heat transfer rate) and with the marked differences in transition position.

There is also considerable difficulty in defining temperatures representative of the laminar boundary layer before transition, because of the limited number of thermocouple positions and the fact that no measurements were available upstream of a station 2½ inches from the tip.

So the representative laminar temperature was arbitrarily chosen to be that measured at x = 2½ inches on the top generator. (Once again, an error of 3°C would correspond to 0.01 in T_w/T_{wo}.)

4.2 Transition results from shadowgraph pictures

These are given in Fig.15 as plots of transition Reynolds number (based on local conditions appropriate to zero incidence) against the ratio T_w/T_{wo}, where T_w is the surface temperature at x = $2\frac{1}{2}$ inches and T_{wo} is the zero heat transfer temperature for a laminar boundary layer, assuming a recovery factor of 0.85 and zero incidence flow conditions.

The results for M_∞ = 1.97 and p_o = 3 atmospheres in Fig.15a were obtained in two distinct tests and have been denoted accordingly because of apparent differences in zero heat transfer transition Reynolds numbers. (A zero heat transfer condition was not obtained in Test K.)

The results at M_∞ = 3.01 and p_o = 4 atmospheres (Fig.15b) are too few in number to justify the drawing of mean curves.

The interesting result from Figs.15a and 15b is that while transition Reynolds number on the bottom generator increased, with decreasing T_w/T_{wo}, at about the same rate as was found in the tests at zero incidence (shown by the mean curves from Figs.11a and 12a for α = 0), there was little, if any, movement on the top generator.

This indicates that the cross-flows engendered by incidence may dominate the scene on the leeward (top) surface and, if this is the case, it would be very important to keep the effective incidence and yaw of a body of revolution close to zero if extensive runs of laminar boundary layer were desired. The limits to be set on incidence and yaw would depend on the cone angle: thus Ref.6 verifies that α/θ is the relevant factor (where, as in theoretical treatments, θ is the semi-angle of the cone) and in the present case an incidence of 2°, giving α/θ = 0.267 could be too large.

The conditional clauses in the previous paragraph are dictated by the fact that transition on the top (leeward) generator was not easily determined, since it was within three inches of the cone tip, where the boundary layer was of the same order of thickness as the diffraction fringe on the shadowgraph pictures. Thus there may have been small movements which were not detected in the photographs. Time did not permit check tests to be made at lower stagnation pressures (giving larger values of x_T) but this will be done during the tests at R.A.E./Farnborough.

5 Conclusions

Measurements of boundary layer transition (using shadowgraph pictures) on a 15° cone in a wind tunnel at M_∞ = 1.97 and 3.01 led to the following conclusions when the cone was at zero incidence relative to the centre line of the tunnel.

(1) Under zero heat transfer conditions at M_∞ = 1.97, the transition Reynolds number stayed constant over a range of stagnation pressures (p_o) from 2 to 3 atmospheres. The values were about 4.5 million on the top and 3.9 million on the bottom generator of the cone (Fig.10a). The difference may have been caused either by a small angle of incidence relative to the airstream or by disturbed flow over the forward portion of the cone (Fig.7a).

(2) However at M_∞ = 3.01, the transition Reynolds number increased roughly linearly from about 3 million at p_o = 2 atmospheres to about 4 million at p_o = 4 atmospheres (Fig.10b). An adverse pressure gradient over the rear of the cone (Fig.7b) may provide the explanation of this anomaly. The difference between values on top and bottom generators was smaller than at M_∞ = 1.97.

(3) When the cone was cooled, the variation of transition Reynolds number with surface temperature at $M_\infty = 1.97$ was less than would be given by the mean correlation curve of Ref.5, which was based on results in the range $1.5 < M < 2.5$, (Fig.11c). However, the differences are not considered to be unduly significant in view both of the disturbed flow over the front of the cone (Fig.7a) and of the errors involved in defining a surface temperature representative of the laminar boundary layer ahead of transition, from temperature distributions such as in Fig.9.

(4) Cooling was less effective in delaying transition when the tunnel Mach number was raised to 3.01. Alternative analyses of the test results were possible because of the dependence of transition under zero heat transfer conditions on stagnation pressure and hence on distance from the tip of the cone (Figs.7b and 13a). The results of these analyses are given in Fig.13b and show, for example, that when $T_w/T_{wo} = 0.9$, R_T/R_{T_o} was reduced from 1.6 at $M_1 = 1.86$ ($M_\infty = 1.97$) to between 1.19 and 1.32 at $M_1 = 2.81$ ($M_\infty = 3.01$).

When the cone was set at 2^o of positive incidence the following result was found.

(5) Both at $M_\infty = 1.97$ and 3.01, transition on the bottom (windward) generator moved aft with cooling at about the same rate as was found in the zero incidence tests. However, there was little, if any, movement of the transition point on the top (leeward) generator (Fig.15) which would indicate that the cross-flows set up by incidence may be the dominant factor in determining transition on the leeward surface.

This conclusion is not as firm as it might be, because when the incidence was 2^o, transition on the top (leeward) generator was not easy to determine from the shadowgraph pictures, since it was within three inches of the cone tip, and the boundary layer was of the same order of thickness as the diffraction fringe in the photograph. Tests at lower stagnation pressure would remove this difficulty (since transition would be further back) and these will be included in the tests to follow at R.A.E./Farnborough.

LIST OF SYMBOLS

M Mach number

M_∞ Mach number in working section of tunnel, ahead tip shock wave of cone

M_1 local Mach number outside boundary layer on cone surface

p_o stagnation pressure absolute (atmospheres)

r temperature recovery factor $= \dfrac{T_{wo} - T_1}{T_{H1} - T_1}$, where T_1 is static temperature of stream outside boundary layer, T_{wo} and T_{H1} are defined below

R_T transition Reynolds number based on local flow conditions $= u_1 x_T/\nu_1$, where u_1 and ν_1 are the velocity and kinematic viscosity of the stream outside the boundary layer, and x_T is defined below

R_{T_o} transition Reynolds number under zero heat transfer conditions, again based on local conditions $= u_1 x_{T_o}/\nu_1$, where x_{T_o} is defined below

LIST OF SYMBOLS (Contd.)

T_{H1}	stagnation temperature, equal to total temperature outside boundary layer	(^{o}K or ^{o}C)
T_{w}	temperature of cone surface	(^{o}K or ^{o}C)
T_{wo}	value of T_{w} under zero heat transfer conditions	(^{o}K or ^{o}C)
x	distance from tip along generator of cone	(inches)
x_{T}	value of x at the transition point from laminar to turbulent flow	(inches)
α	incidence of axis of cone relative to centre line of tunnel (more strictly should be relative to airstream)	(degrees)
θ	semi-angle of cone ($7\frac{1}{2}^{o}$ in present tests)	(degrees)
δ	boundary layer thickness	
e	maximum depth of a surface discontinuity	

REFERENCES

No.	Author	Title, etc.
1	L. Lees	The stability of the laminar boundary layer in a compressible fluid. NACA Report 876, 1947.
2	E.R. Van Driest	Calculation of the stability of the laminar boundary layer in a compressible fluid on a flat plate with heat transfer. Journal of the Aeronautical Sciences, Vol.19, p.801. December 1952.
3	D.W. Dunn and C.C. Lin	On the stability of the laminar boundary layer in a compressible fluid. Journal of the Aeronautical Sciences, Vol.22, P.455. July 1955.
4	M. Morduchow, R.G. Grape	Separation, stability and other properties of compressible laminar boundary layers with pressure gradients and heat transfer. NACA Technical Note No.3296, May 1955.
5	R.J. Monaghan	A survey and correlation of data on heat transfer by forced convection at supersonic speeds. R & M 3033, September 1953.
6	F.V. Davies and R.J. Monaghan	Boundary layer measurements on 15° and 24.5° cones at small angles of incidence at M = 3.17 and 3.82 and zero heat transfers. RAE Report No. Aero.2577, 1957.
7	J.F.W. Crane and A.C. Browning	A comparison between several methods of detecting boundary layer transition in high speed flow. RAE Technical Note Aero. (to be issued).

REFERENCES (Contd.)

No.	Author	Title, etc.
8	J.F.W. Crane	The use of woollen felt screens as air cleaners in supersonic wind tunnels. RAE Technical Note Aero. (to be issued).
9	G.F. Midwood and R.W. Hayward	An automatic self-balancing capsule manometer. C.P.231, July 1955.
10	W.E. Moeckel	Some effects of bluntness on boundary layer transition and heat transfer at supersonic speeds. NACA Technical Note No.3653, March 1956.
11	J.R. Jack and N.S. Diaconis	Variation of boundary layer transition with heat transfer on two bodies of revolution at a Mach number of 3.12. NACA Technical Note No.3562, September 1955.

APPENDIX I

Thermocouple Installation and Calibration

Details of the thermocouple junctions in the skin of the cone are shown in the inset in Fig.4. Each junction was formed by Easiflow brazing a 35 S.W.G. enamelled and glass covered constantan wire and protective 1 mm stainless steel tube into a mild steel button, whose thickness was equal to the skin thickness. The technique used in brazing was to apply heat and brazing material to the blind hole in the steel button, and then to plunge the stainless steel tube and wire (with the end of the wire bared and just proud of the tube) into the blind hole. By this means a near surface junction can be obtained. (A check on each thermocouple for correct junction was made before installation in the skin.) The button joint with the cone skin was made with soft solder, and the correct contour at the surface was obtained by a process of hand filing and scraping and of lathe polishing. Profiles of the joints obtained are given in Fig.5a.

Laboratory tests have shown that this type of thermocouple records faithfully the skin temperature at fairly large rates of heat transfer. Calibration of the wire used was made with the tunnel temperature measuring equipment and a lagged tank of well stirred alcohol cooled by solid carbon dioxide. Three sample thermocouples were attached to the bulb of an alcohol thermometer graduated in $0.1^{\circ}C$, and e.m.f. values at intervals of one degree Centigrade from $-60^{\circ}C$ to $+20^{\circ}C$ were taken. A check on the alcohol thermometer was made at the freezing point of mercury; there was no error. In addition a standard thermocouple of Platinum versus Platinum/13% Rhodium was used to calibrate the scale between the upper limit of the alcohol thermometer at $0^{\circ}C$ and the "Cold Junction" thermostat temperature of $+41^{\circ}C$. Repeat calibration at a later date produced identical results.

APPENDIX II

Model Cooling Apparatus

The model cooling system, detailed in Fig.6 and shown in the experimental arrangement in Fig.2, uses methyl alcohol as a heat transport fluid and methyl alcohol cooled by CO_2 solid as a cold sink. The heat transport fluid is blown through the model by means of pressure air, preferably of dry tunnel air, and the circulation is maintained by an electrically driven gear pump. By this means a gaseous free flow is achieved.

From the header tank, which is vented to atmosphere, the circulating fluid is pumped (by a gear pump driven by a D.C. electric motor with speed control) to a gallery. Three outlets from the gallery pipe are provided, each with an adjustable valve. The first is a return to the header tank, the second leads to the inlet side of the cooling coil, and the third is to a cooler by-pass line to the de-aerator.

By means of these three valves the coolant may be:-

(a) short-circuited back to the header tank

(b) passed through the cooler

(c) passed straight to the de-aerator

(d) mixed to obtain a steady heat flow rate by means of a combination of (b) and (c).

The cooler consists of a doubly wound coil of copper tube suspended in a drum containing about 8 gallons of cold alcohol. This alcohol is cooled by the addition of CO_2 solid which must be administered carefully to limit the gassing rate. The drum is mounted in a wooden case and is insulated with granulated cork.

The de-aerator consists of a steel drum with a detachable lid which contains connections for the coolant and pressure air. On entry the coolant is directed towards the wall of the de-aerator to avoid the formation of bubbles which occur with a direct jet into a standing tank of fluid. The outlet for the coolant is through a bell-mouth stack pipe positioned with its entry one inch above the base of the tank, and coolant is forced up this pipe by means of air pressure.

Pressure air connections are in the lid and adjustable valves on both the inlet and bleed provide delicate control of the airflow through and pressure in the de-aerator. By adjustment of these valves in conjunction with the pump speed, a constant coolant level in the de-aerator may be maintained (the level is shown on a sighting glass), and an extremely steady flow rate established.

Between the de-aerator and the model a by-pass to the header tank is fitted which enables the system and not the model to be cooled, and by this means the system may be reduced in temperature to $-60^{\circ}C$ before a tunnel test, without formation of ice on the model. From room temperature this takes about an hour to accomplish.

Initially the circuit through the cone was by way of drillings in the wedge beam support, but this was abandoned in favour of improved cooling through the insulated copper pipes shown in Fig.3. These pipes connect with two drillings in the cone sting, Fig.4. One drilling is concentric with a copper pipe running centrally to the cone tip which issues or accepts

coolant at that point, thus ensuring maximum cooling in the tip region. At the base of the cone four small drillings spaced widely apart connect with the second drilling in the sting and complete the coolant circuit through the cone. Both sting drillings accommodate steel/constantan thermocouples for the measurement of inlet and outlet coolant temperatures. Vent pipes are provided in the base of the cone and a regulated drip feed into a glass beaker gives a visual indication of the flow condition.

The outlet from the cone is via a flexible pipe to a Rotameter flowmeter. This has been calibrated over a wide band of temperatures and registers flow rates of between 100 and 550 pints/hr. From the Rotameter the coolant passes into the header tank via a two-way cock. A sighting glass is provided on the header tank and is used in conjunction with a similar one on the de-aerator to observe the balancing of flow through the system.

When operating the rig it is a general practice to cool the model down to the lowest desired or possible temperature, and to hold this constant by a process of graduated feed of CO_2 solid to the cooler, or by method (d). Step increases in temperature are obtained by by-passing the cooler (method (c)), thus allowing the tunnel to warm up the heat transport fluid, by adding warm alcohol, or by a combination of both.

For tests at zero heat transfer the complete elimination of coolant from the model may be obtained by blowing out with all gallery valves closed and the pump switched off.

APPENDIX III

Surface condition in the neighbourhood of Thermocouple junctions on the heat transfer cone

Magnified profiles of two thermocouple junctions near the tip are shown in Fig. 5a. The profile A is of a typical junction and is situated on the bottom generator at x = 3.1 inches (where x is the slant distance from the tip). This order of surface discontinuity had no effect on transition, by comparison with the results obtained at zero heat transfer with the 15° stainless steel cone, using both azo-benzene and optical methods of transition measurement.

The profile B is of a damaged thermocouple junction which fixed transition on the top generator at its location (x = 2.6 inches) for the range of pressures p_o = 1 to 4 atmospheres (M_1 = 2.81). The profile C, which is of this same junction after repair, had no effect on transition.

A comparison of the ratio $^e/\delta$, the maximum surface discontinuity divided by the theoretical local laminar boundary layer thickness, is tabulated below and suggests a critical value of 0.048 for no effect on transition under these operating conditions. The values for δ were obtained from the formula

$$\delta = 6\,(1 + 0.0795\,M_1^2)\ \times\ (R_x)^{-\frac{1}{2}}\ (3)^{-\frac{1}{2}}\ .$$

Surface Profile Fig.	M_1	x (inches)	p_o (atmospheres)	δ (inches)	e (inches)	$^e/\delta$	Effect on transition
a	2.81	3.1	1	0.0229	0.0005	0.0218	Nil
a	"	"	4	0.01145	0.0005	0.0437	Nil
b	"	2.6	1	0.0209	0.001	0.0479	Fixed at x
b	"	"	4	0.01055	0.001	0.0955	Fixed at x
c	"	"	1	0.0209	0.0005	0.0239	Nil
c	"	"	4	0.01045	0.0005	0.0479	Nil
c	1.86	"	1	0.021	0.0005	0.0238	Nil
c	"	"	3	0.01215	0.0005	0.0411	Nil

TABLE I

Test results showing effect of cooling on transition at zero incidence (as determined by shadowgraph)

1 $M_\infty = 1.97$, $(M_1 = 1.86)$, $p_o = 3$ atmospheres.

T_{wo}/T_{H1} assumed to be 0.939 (corresponding to a laminar recovery factor of 0.85).

(a) Coolant flowing from base to tip of cone

Test	T_{wo} °K	T_w °K x=2½ in.	R_T millions Top generator	R_T millions Bottom generator	T_w/T_{wo} x=2½ in.	T_w/T_{wo} inflexion
A	294	255.5	> 7.57	7.07	0.869	0.882
	294	256.4	7.57	6.89	0.872	0.884
B	293	251.1	> 7.57	> 7.57	0.857	0.871
	294.5	256.0	7.34	-	0.870	0.882
	294.5	260.6	6.89	6.24	0.885	0.895
	295	264.1	6.61	6.15	0.895	0.904
C	292	270.3	5.51	4.77	0.927	0.933
	294	276.5	5.23	4.59	0.941	0.946
	294.5	282.1	5.05	4.32	0.958	0.961
	294.5	287.6	4.77	4.32	0.977	0.979
	295	294	4.41	3.86	0.997	0.998

(b) Coolant flowing from tip to base of cone

						Top	Bottom
D	292.5	242.0	6.79	7.25	0.827	0.871	0.849
	294.5	269.4	5.69	5.23	0.915	0.915	
						Top	Bottom
E	290.5	242.7	6.89	7.07	0.836	0.867	0.856
	294	259.4	6.15	6.33	0.882	0.892	0.887
	294	278.4	4.77	4.22	0.947	0.947	
	294	283.4	4.59	4.04	0.964	0.964	
	294	286.2	4.41	3.67	0.973	0.973	
	294	294	4.32*	3.49*	1.000	1.000	

* Taken to be 4.1 and 3.4 when evaluating R_T/R_{T_o} in Fig.11c, since these values agree better with the trends shown by the results with cooling $(T_w/T_{wo} < 1)$.

TABLE I (Contd.)

2 $M_\infty = 3.01$, $(M_1 = 2.81)$, $p_o = 4$ atmospheres.

T_{wo}/T_{H1} assumed to be 0.908 (corresponding to a laminar recovery factor of 0.85).

(a) Coolant flowing from base to tip of cone

Test	T_{wo} °K	T_w °K $x=2\frac{1}{2}$ in.	R_T millions Top generator	R_T millions Bottom generator	T_w/T_{wo} $x=2\frac{1}{2}$ in.	T_w/T_{wo} inflexion
F	282	242.4	5.44	-	0.859	0.869
	282.5	244.3	5.36	4.91	0.865	0.874
	282.5	246.9	5.14	4.68	0.874	0.882
	282.5	250.8	5.14	4.76	0.888	0.896
	282.5	261.3	4.76	4.53	0.925	0.930
	282.5	272.2	4.53	4.23	0.963	0.963
G	282.5	239.4	5.67	5.29	0.847	0.857
	283	249.7	5.14	4.76	0.883	0.891
	283	254.9	5.14	4.68	0.901	0.908
	283	261.4	4.91	4.38	0.924	0.929
	283.5	266.4	4.68	4.38	0.940	0.942
	283	271.3	4.68	4.31	0.959	0.959
	283	276.9	4.53	4.16	0.979	0.978
	283	284	4.31	4.16*	1.004	1.000

(b) Coolant flowing from tip to base of cone

						Top	Bottom
H	282.5	236.2	5.37	5.44	0.836	0.869	0.847
	283	243.1	5.14	5.06	0.858	0.880	0.867
	283.5	247.8	5.06	4.84	0.875	0.888	0.880
	283.5	255.1	4.98	4.68	0.899	0.900	0.899
	283.5	266.7	4.68	4.38	0.941	0.939	
	282	273.2	4.61	4.23	0.969	0.966	
	282.5	284	4.31	4.23*	1.005	1.000	

* Taken to be 4.05 when evaluating R_T/R_{T_o} in Fig. 12c.

WT.2078.C.P.381-K3 - Printed in Great Britain

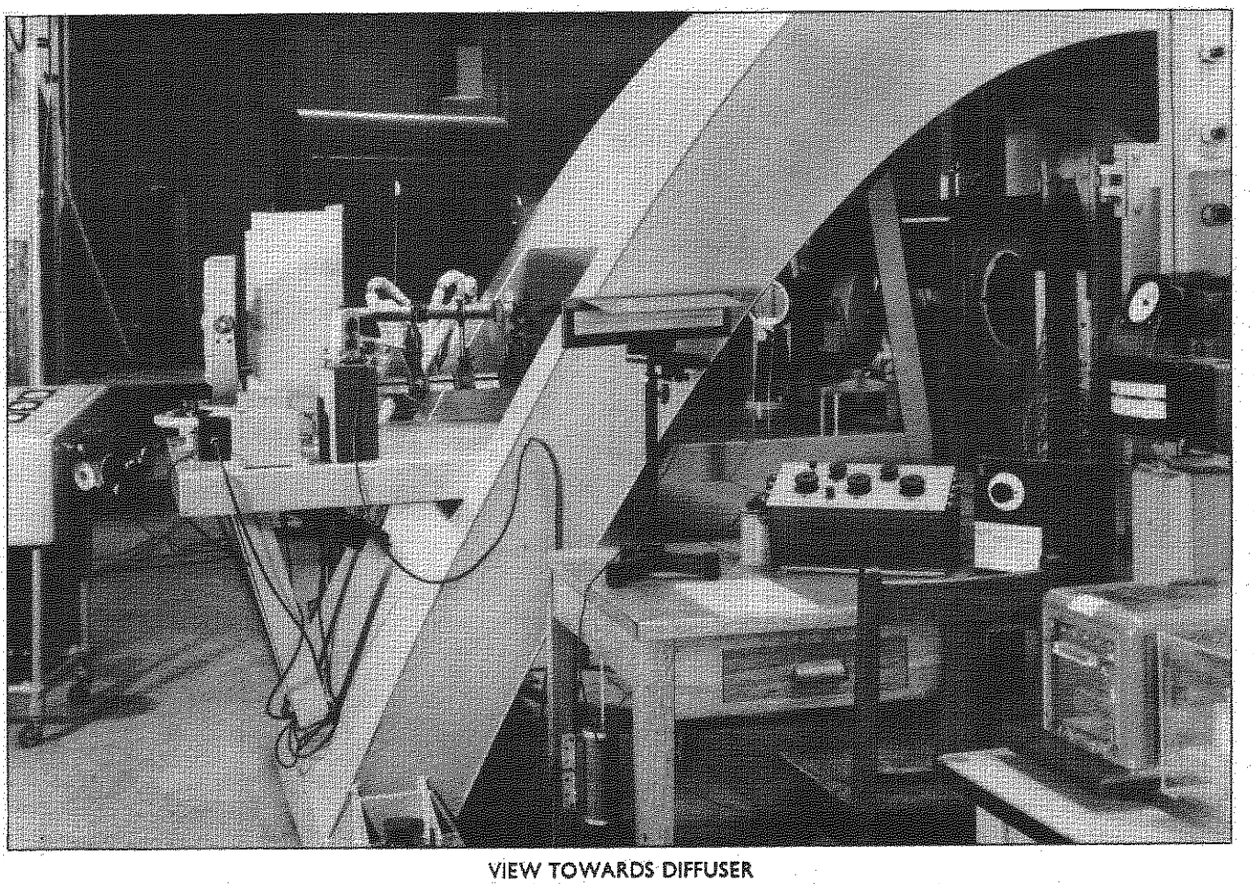

VIEW TOWARDS DIFFUSER

FIG.1. TUNNEL AND EQUIPMENT, SHOWING OPTICAL BRIDGE, AND THERMOCOUPLE POTENTIOMETER

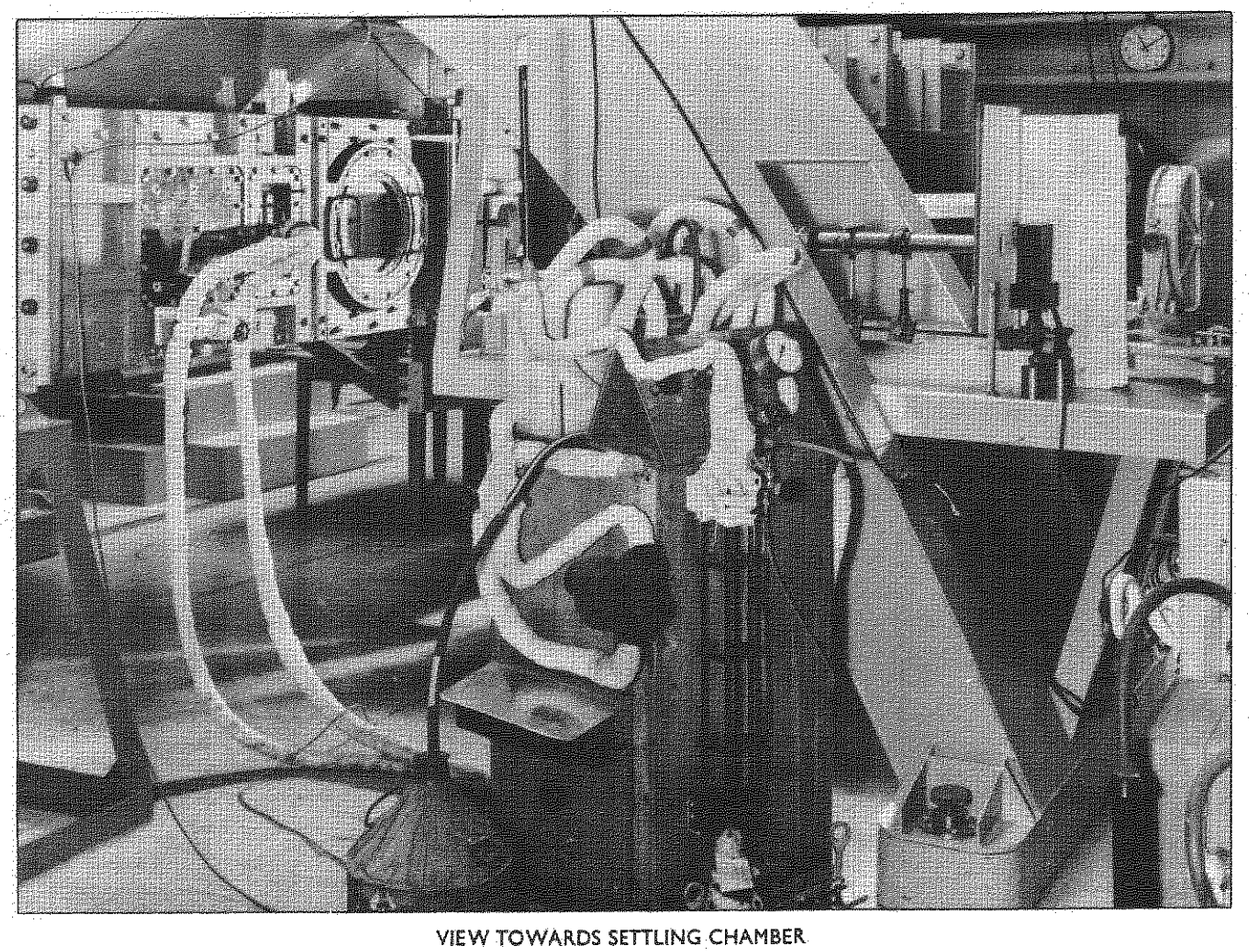

VIEW TOWARDS SETTLING CHAMBER

FIG.2. TUNNEL AND EQUIPMENT, SHOWING THE HEAT EXCHANGER AND COOLANT LINES

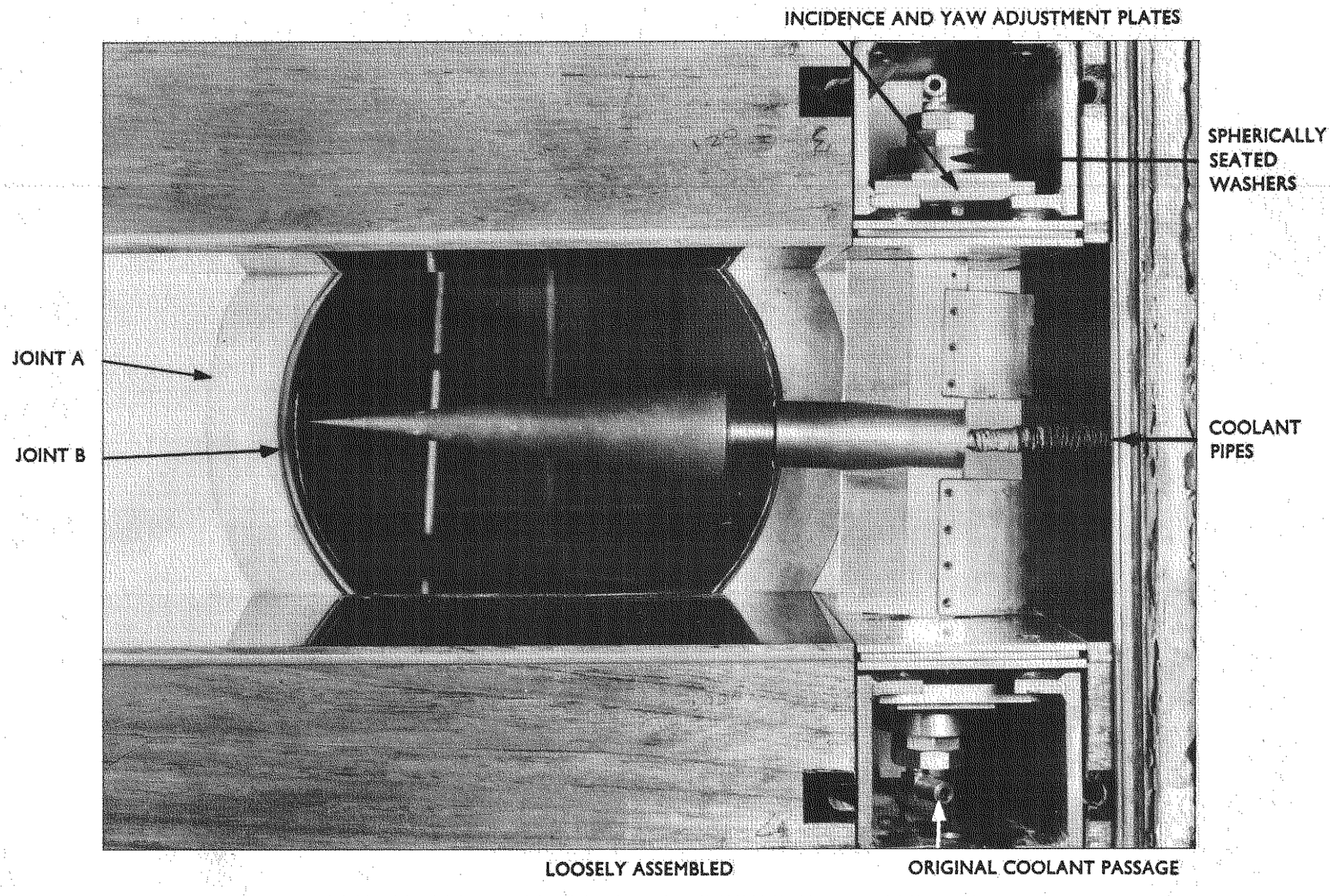

FIG.3. COPPER CONE FOR STATIC PRESSURE MEASUREMENTS, MOUNTED IN THE TUNNEL WORKING SECTION

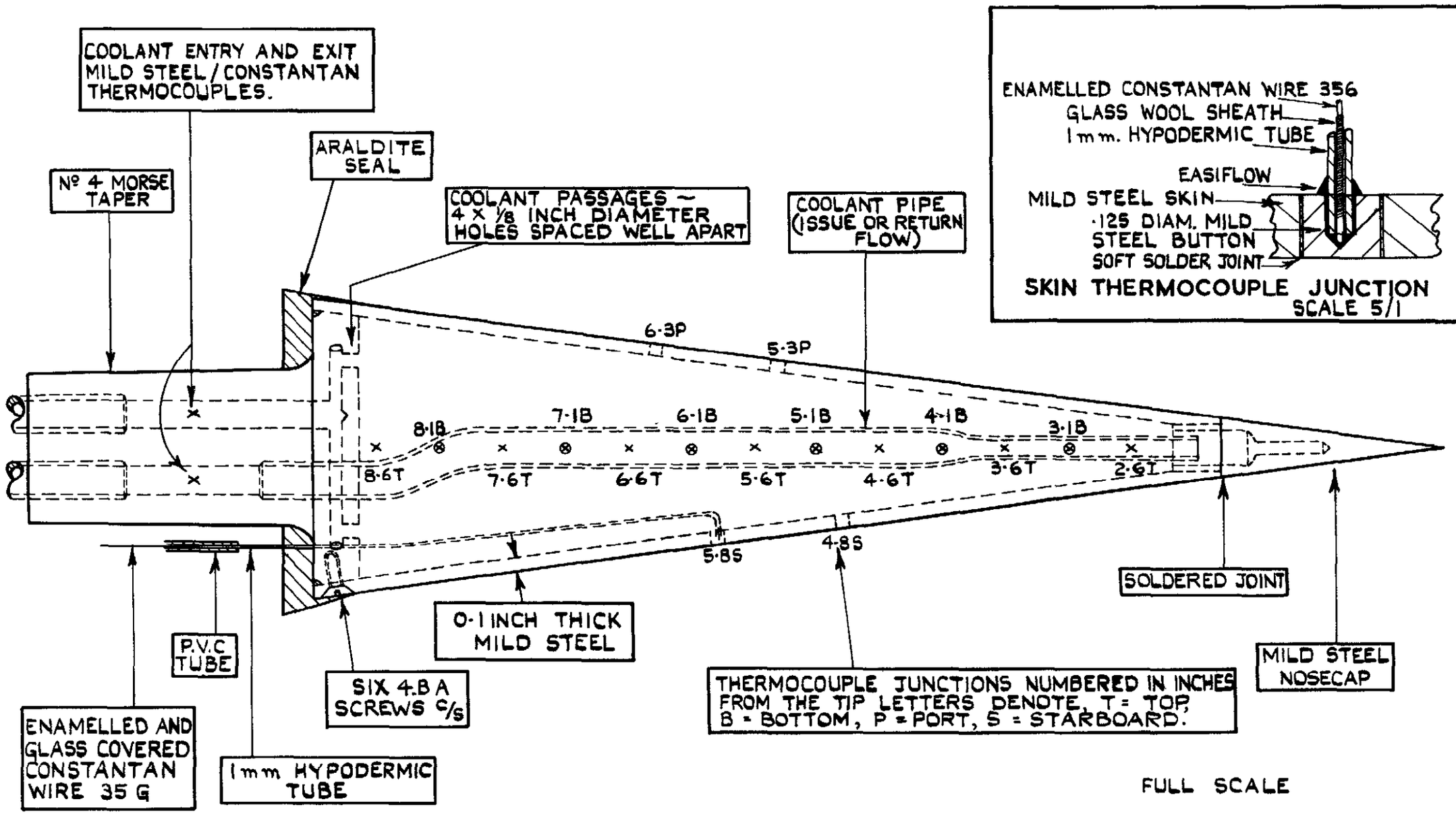

FIG. 4. 15° MILD STEEL HEAT TRANSFER CONE.

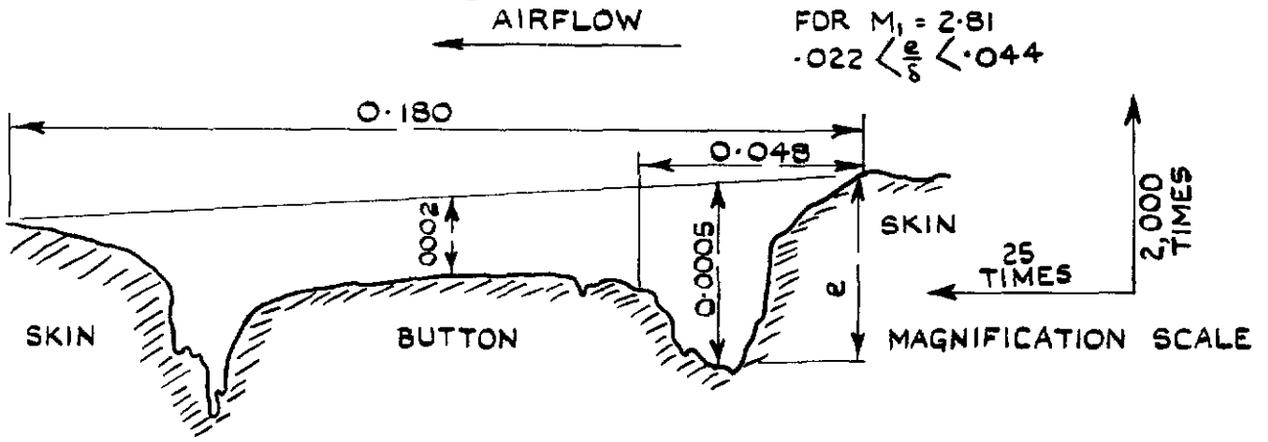

(a) A TYPICAL PROFILE AT 3·1B
NO EFFECT ON TRANSITION

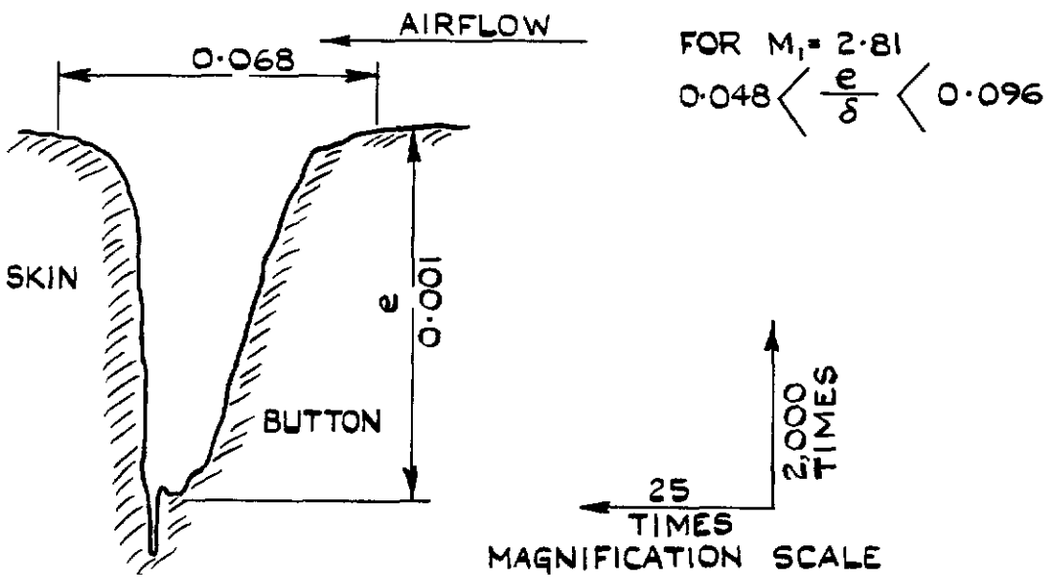

(b) PROFILE OF A DAMAGED THERMOCOUPLE JUNCTION AT 2·6T
THIS FIXED TRANSITION

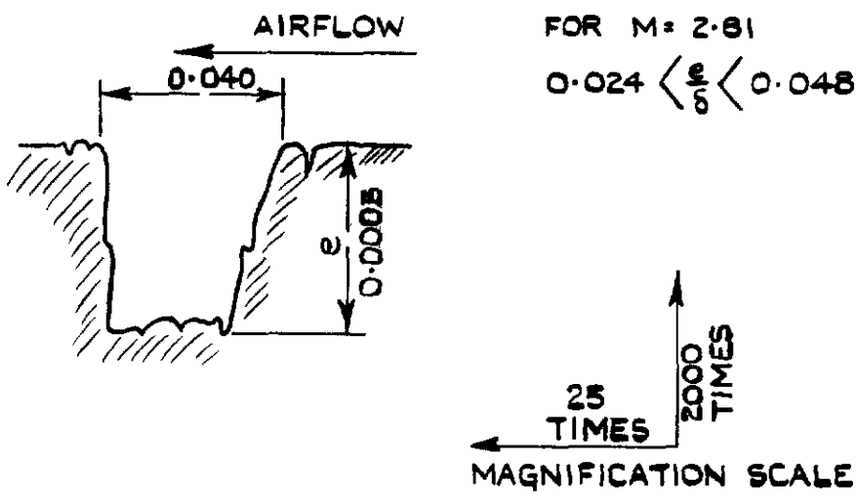

DIMENSIONS IN INCHES

(c) PROFILE OF JUNCTION AT 2·6T AFTER REPAIR
NO EFFECT ON TRANSITION

FIG.5(a-c). PROFILES OF THERMOCOUPLE JUNCTIONS ON THE 15° HEAT TRANSFER CONE.

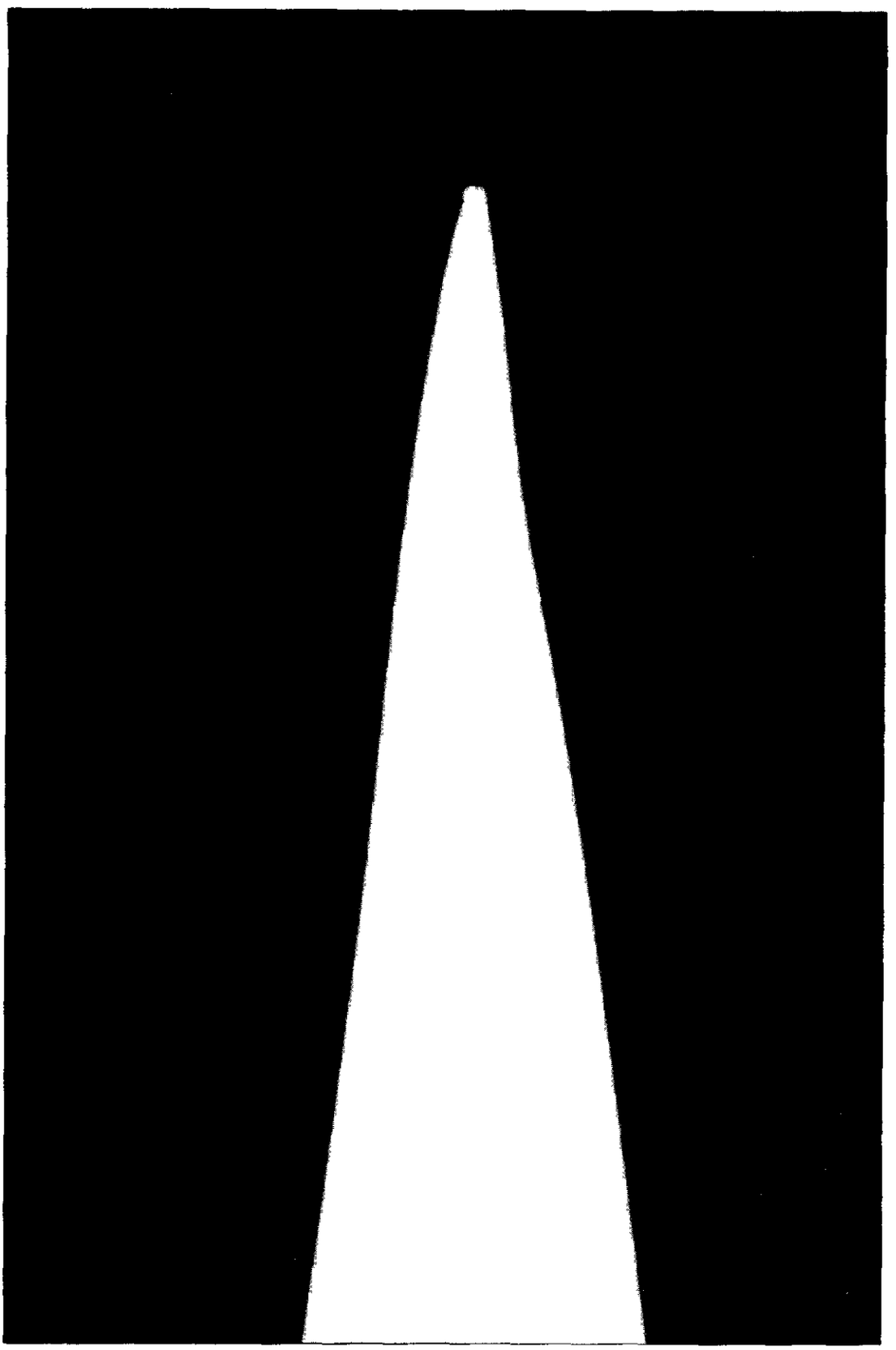

MAGNIFICATION 50

FIG.5b. 15° HEAT TRANSFER CONE TIP, ENLARGED SHADOWGRAPH

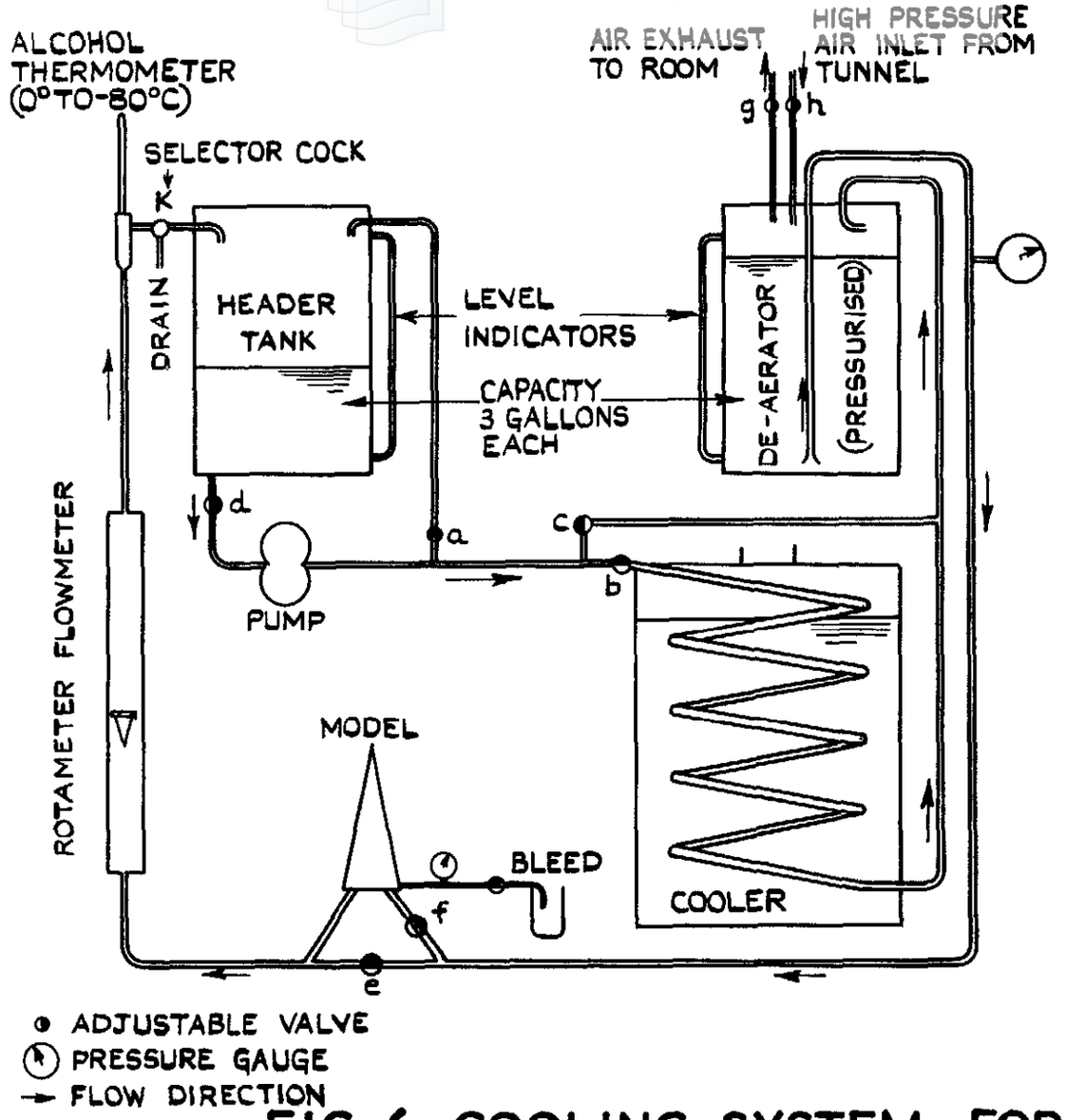

TABLE OF OPERATIONS AND SETTINGS

OPERATION	VALVES OPEN	VALVES CLOSED	CONTROLS
PRIME DE-AERATOR	c d g	a b	PUMP SPEED
COOL SYSTEM	b d e K TO HEADER TANK	a c f	g h PUMP SPEED
CIRCULATE MODEL	d f K TO HEADER TANK	a e	b c g h PUMP SPEED
WARM-UP SYSTEM	c d f K TO HEADER TANK	a b e	g h PUMP SPEED
BLOW-OUT MODEL	f K TO DRAIN OR HEADER TANK	a b c e SWITCH-OFF PUMP	g h

FIG. 6. COOLING SYSTEM FOR WIND TUNNEL MODELS (FULLY DESCRIBED IN APPENDIX II)

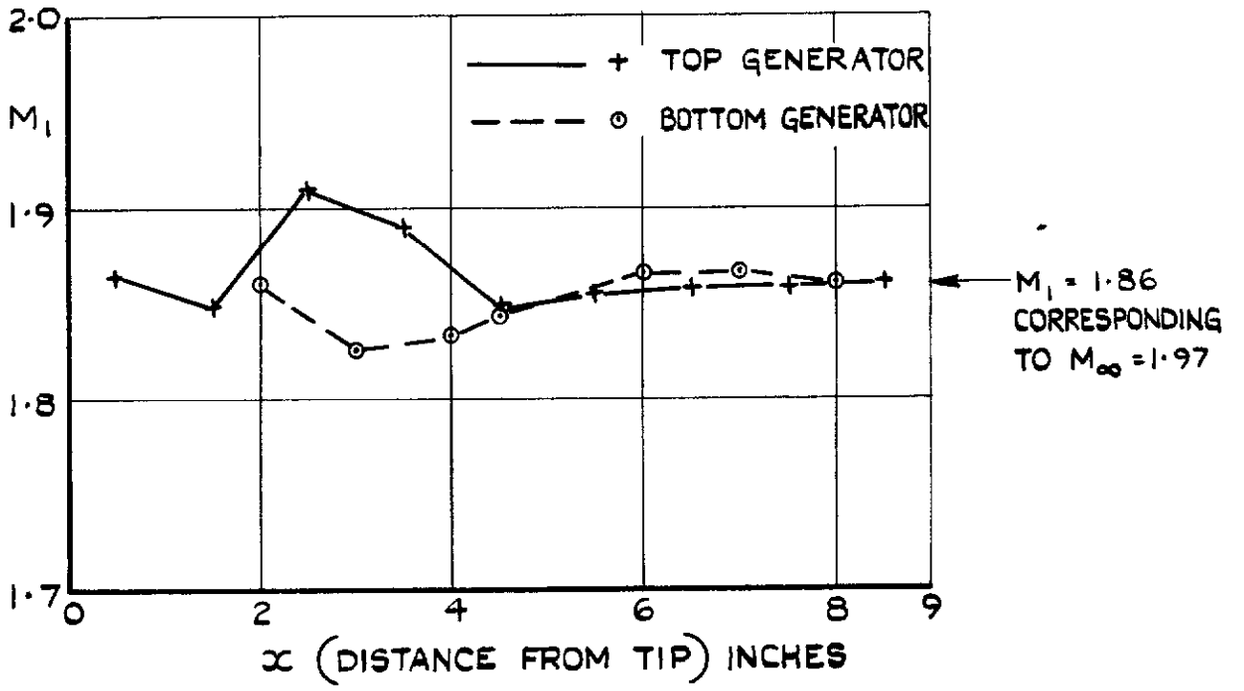

(a) NOMINAL $M_\infty = 2{\cdot}0$ $p_0 = 3$ ATM.

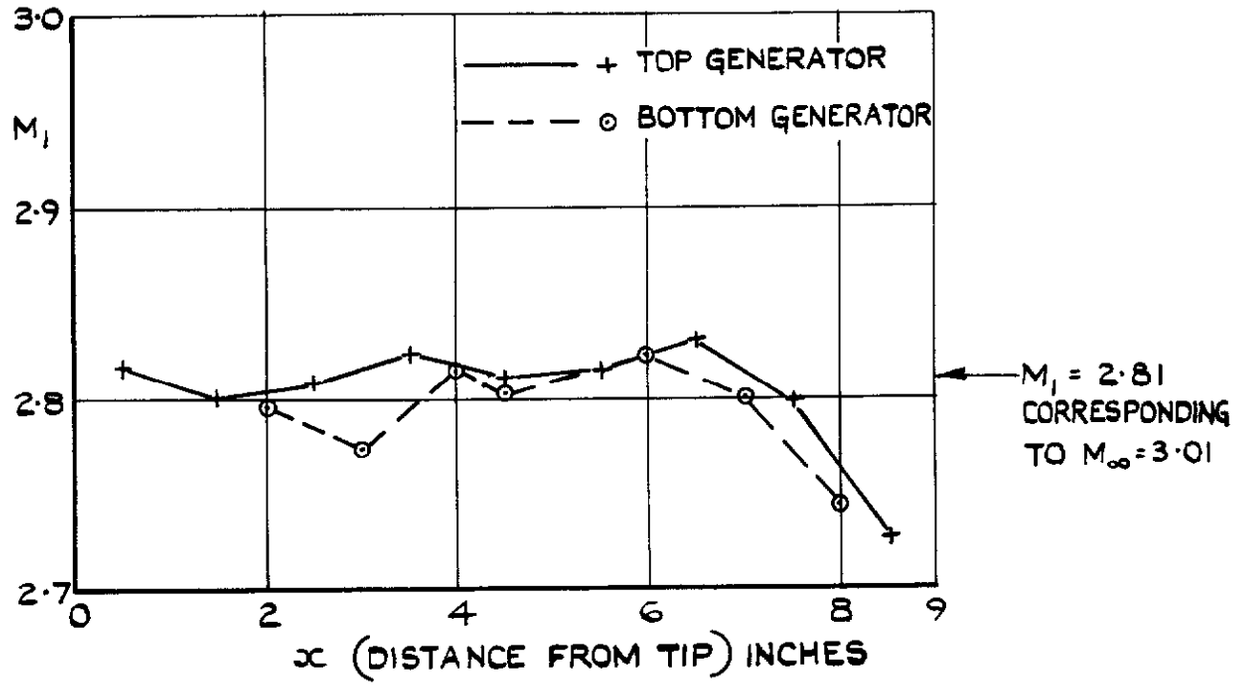

(b) NOMINAL $M_\infty = 3{\cdot}0$ $p_0 = 4$ ATM.

FIG. 7. (a & b). DISTRIBUTIONS OF LOCAL MACH NUMBER (M_1) ALONG THE 15° COPPER CONE FOR NOMINAL TUNNEL MACH NUMBERS (M_∞) OF 2·0 AND 3·0 (ZERO INCIDENCE)

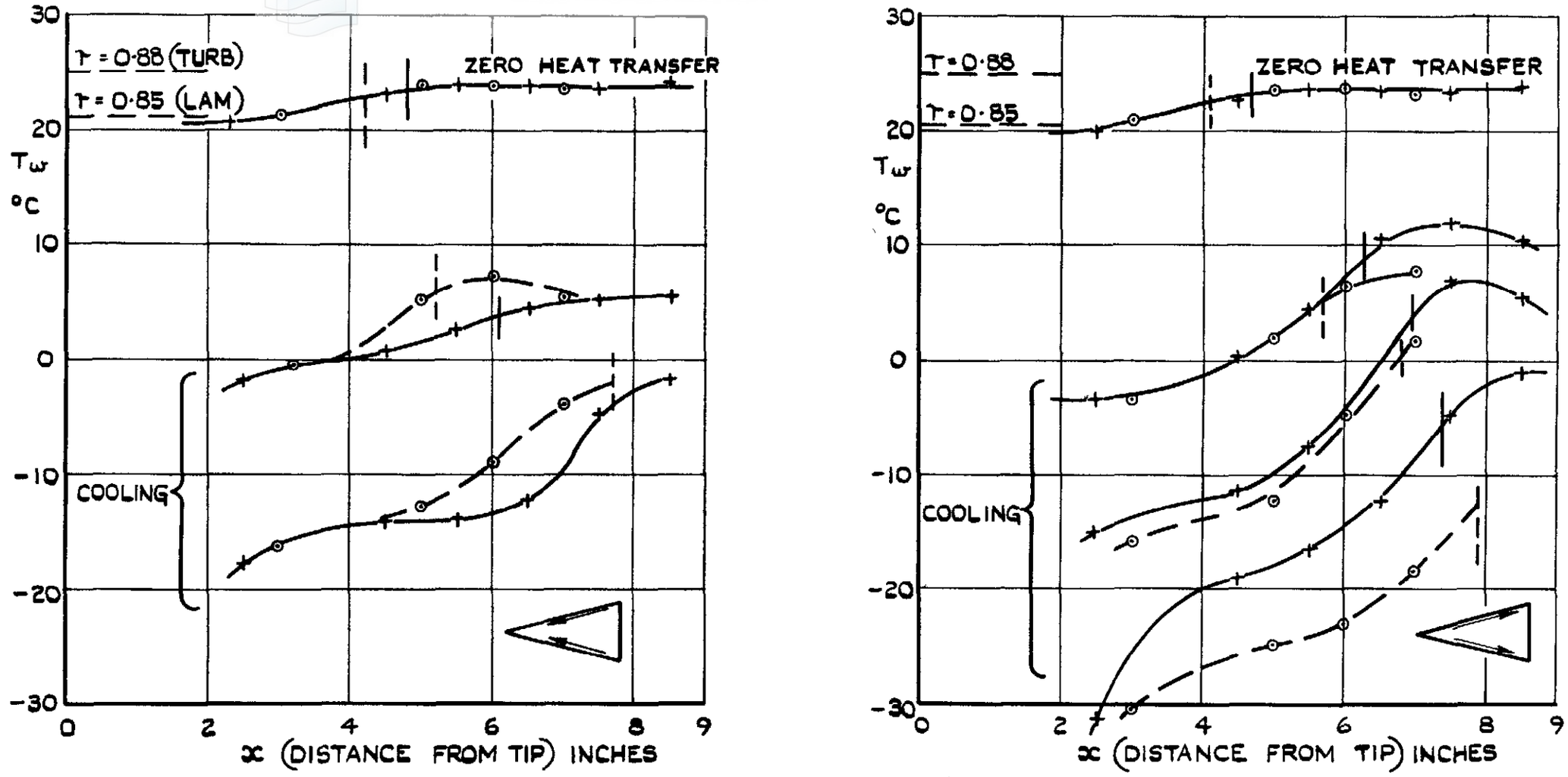

(a) COOLANT FLOWING FROM BASE TO TIP

(b) COOLANT FLOWING FROM TIP TO BASE

FIG.8.(a&b). DISTRIBUTIONS OF SURFACE TEMPERATURE ALONG THE 15° STEEL CONE AT $M_\infty = 1{\cdot}97$ AND $p_0 = 3$ ATM. (ZERO INCIDENCE)

(TRANSITION POSITIONS FROM SHADOWGRAPH SHOWN BY VERTICAL LINES ACROSS CURVES)

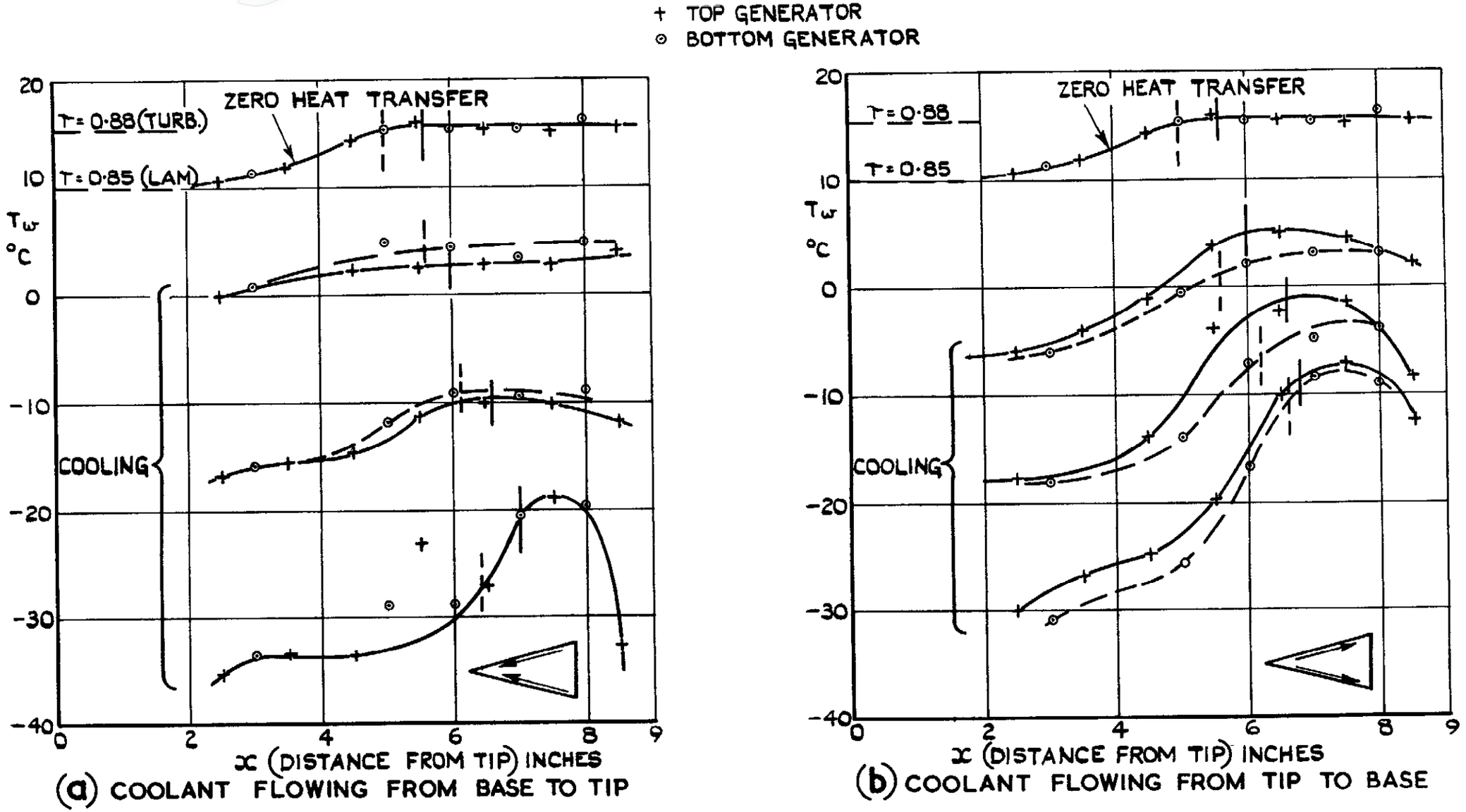

FIG.9.(a&b). DISTRIBUTIONS OF SURFACE TEMPERATURE ALONG THE 15° STEEL CONE AT $M_\infty = 3{\cdot}01$ AND $P_0 = 4$ ATM. (ZERO INCIDENCE)

(TRANSITION POSITIONS FROM SHADOWGRAPH SHOWN BY VERTICAL LINES ACROSS CURVES)

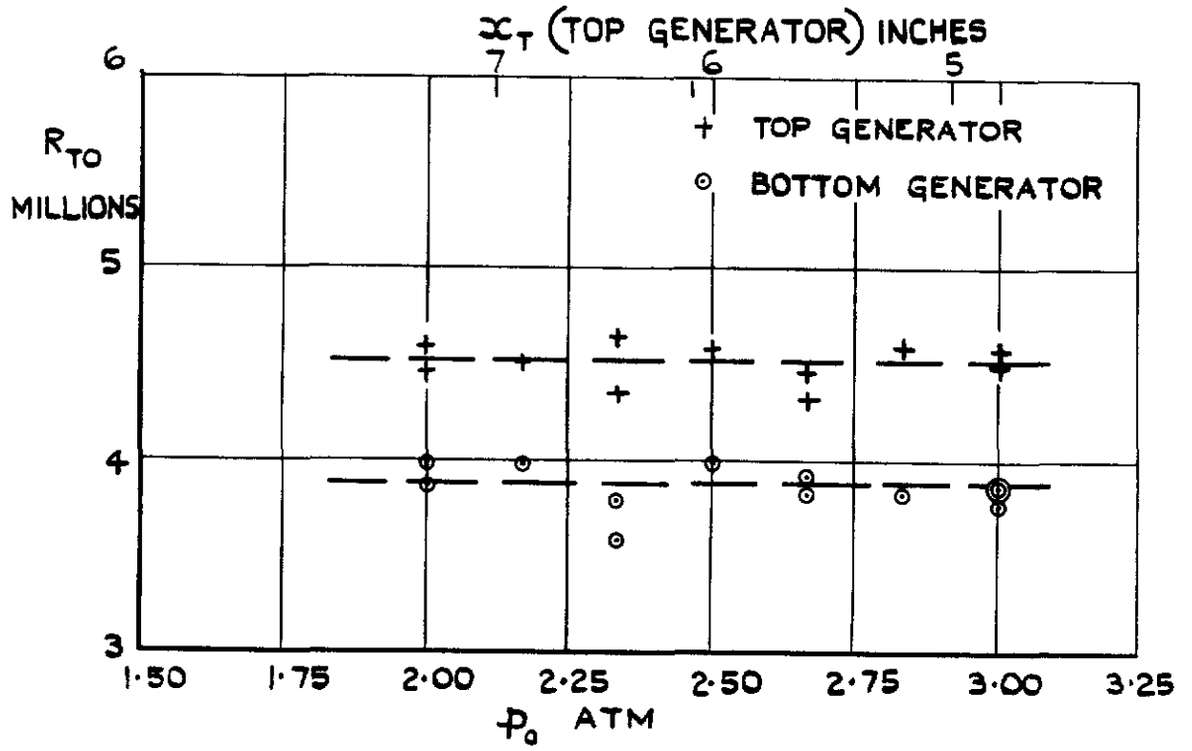

(a) $M_\infty = 1.97$ $(M_1 = 1.86)$

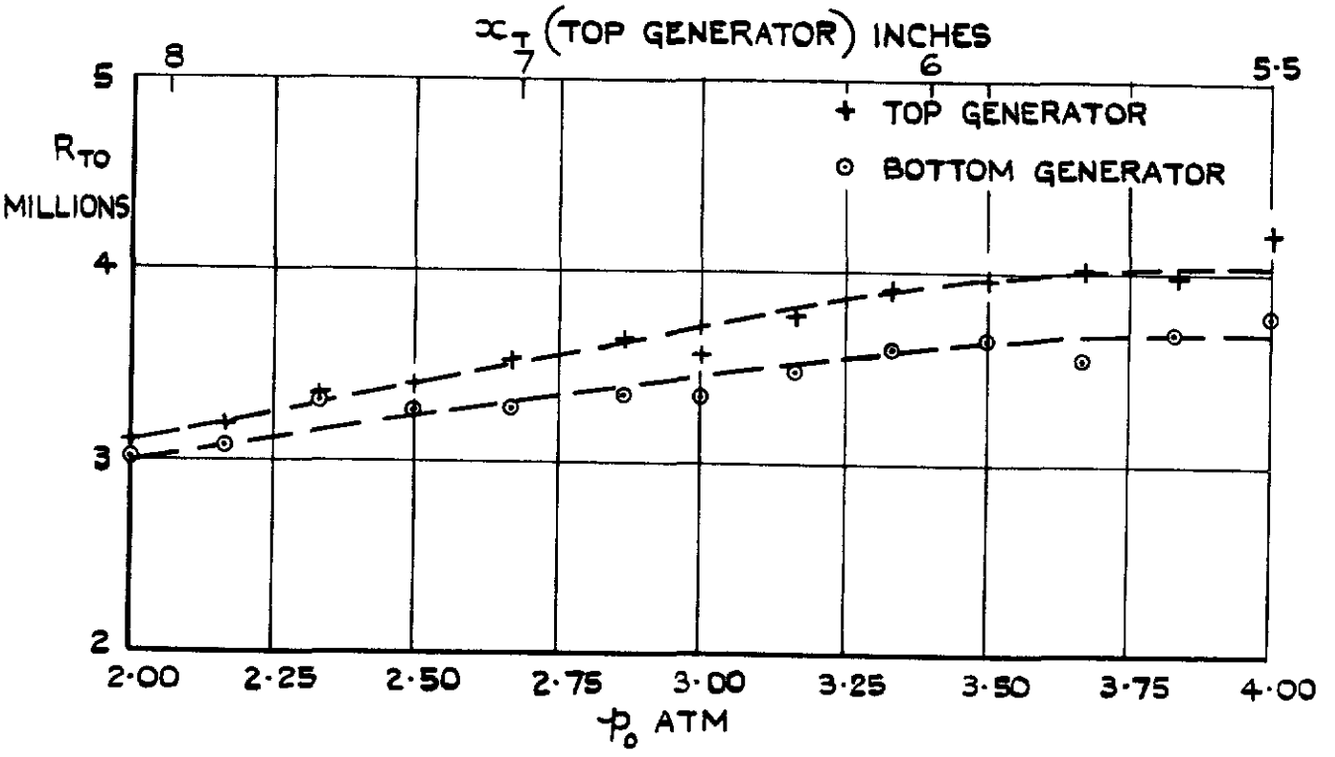

(b) $M_\infty = 3.01$ $(M_1 = 2.81)$

FIG. 10. (a & b). TRANSITION REYNOLDS NUMBERS (FROM SHADOWGRAPH) UNDER ZERO HEAT TRANSFER CONDITIONS (ZERO INCIDENCE)

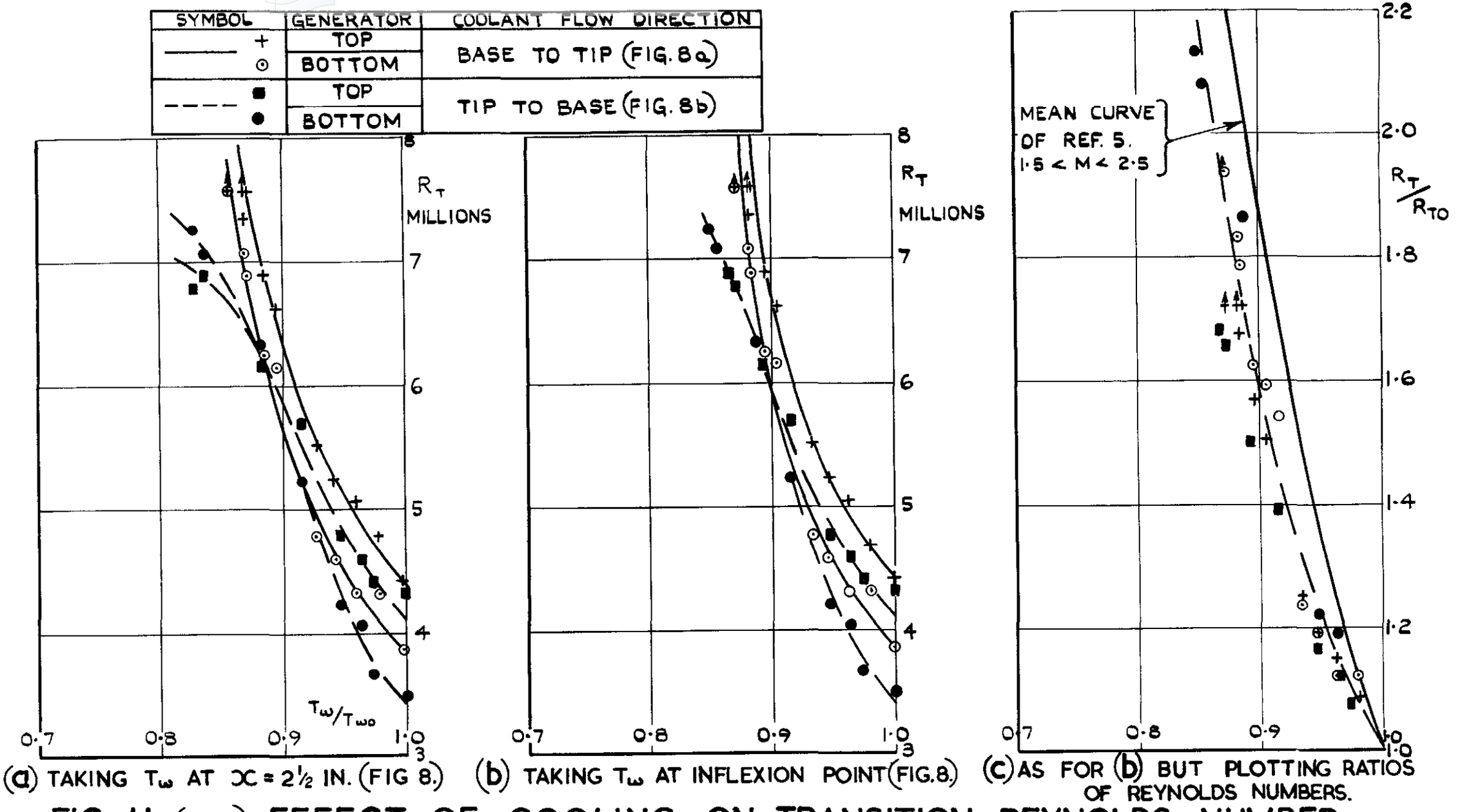

(a) TAKING T_ω AT $x = 2\frac{1}{2}$ IN. (FIG 8.) (b) TAKING T_ω AT INFLEXION POINT (FIG. 8.) (c) AS FOR (b) BUT PLOTTING RATIOS OF REYNOLDS NUMBERS.

FIG. 11. (a-c). EFFECT OF COOLING ON TRANSITION REYNOLDS NUMBER (FROM SHADOWGRAPH) AT $M_\infty = 1{\cdot}97$, ($M_1 = 1{\cdot}86$), AND $P_o = 3$ ATM. (ZERO INCIDENCE)

SYMBOL	GENERATOR	COOLANT FLOW DIRECTION
—— +	TOP	BASE TO TIP (FIG. 9a)
—— ⊙	BOTTOM	
- - - ■	TOP	TIP TO BASE (FIG 9b)
- - - ●	BOTTOM	

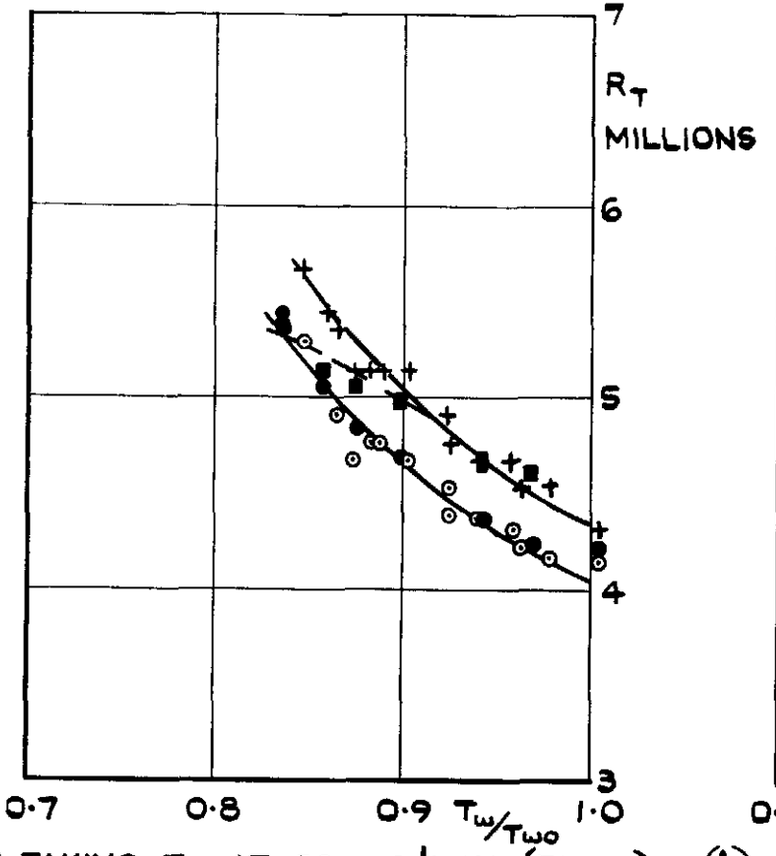

(a) TAKING T_w AT x = 2½ IN. (FIG. 9.)

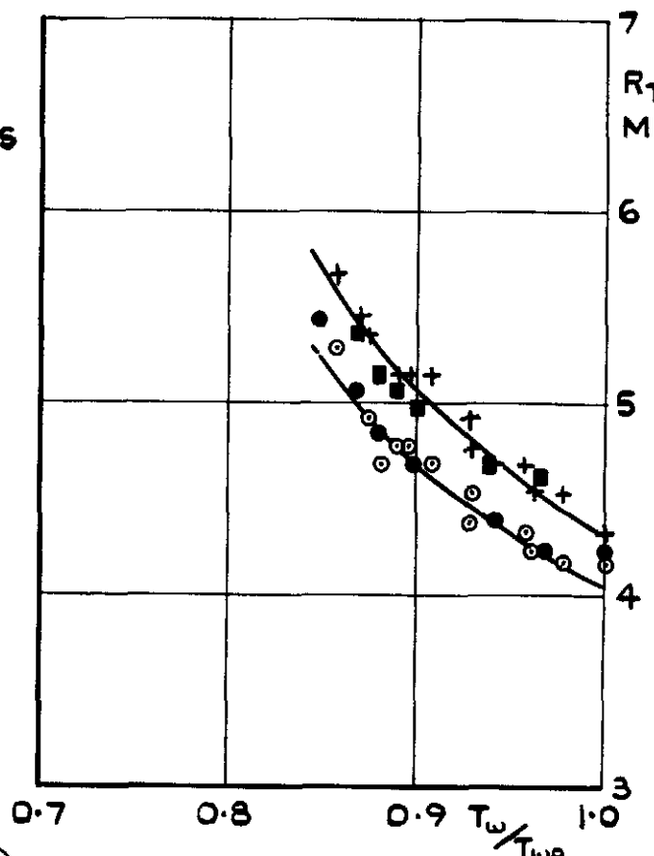

(b) TAKING T_w AT INFLEXION POINT (FIG 9.)

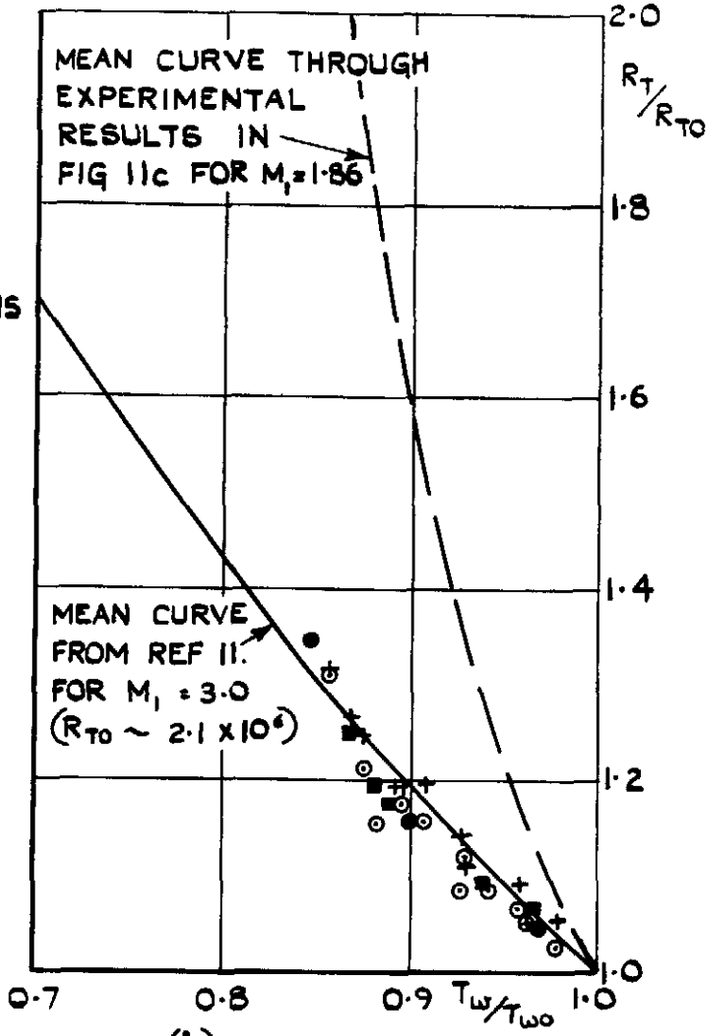

(c) AS FOR (b) BUT PLOTTING RATIOS OF REYNOLDS NUMBERS.

FIG. 12.(a-c). EFFECT OF COOLING ON TRANSITION REYNOLDS NUMBER (FROM SHADOWGRAPH) AT M_∞ = 3·01, (M_1 = 2·81), AND p_o = 4 ATM. (ZERO INCIDENCE)

EXPERIMENTAL RESULTS ARE FOR TOP GENERATOR ONLY AND WITH COOLANT FLOWING FROM BASE TO TIP.

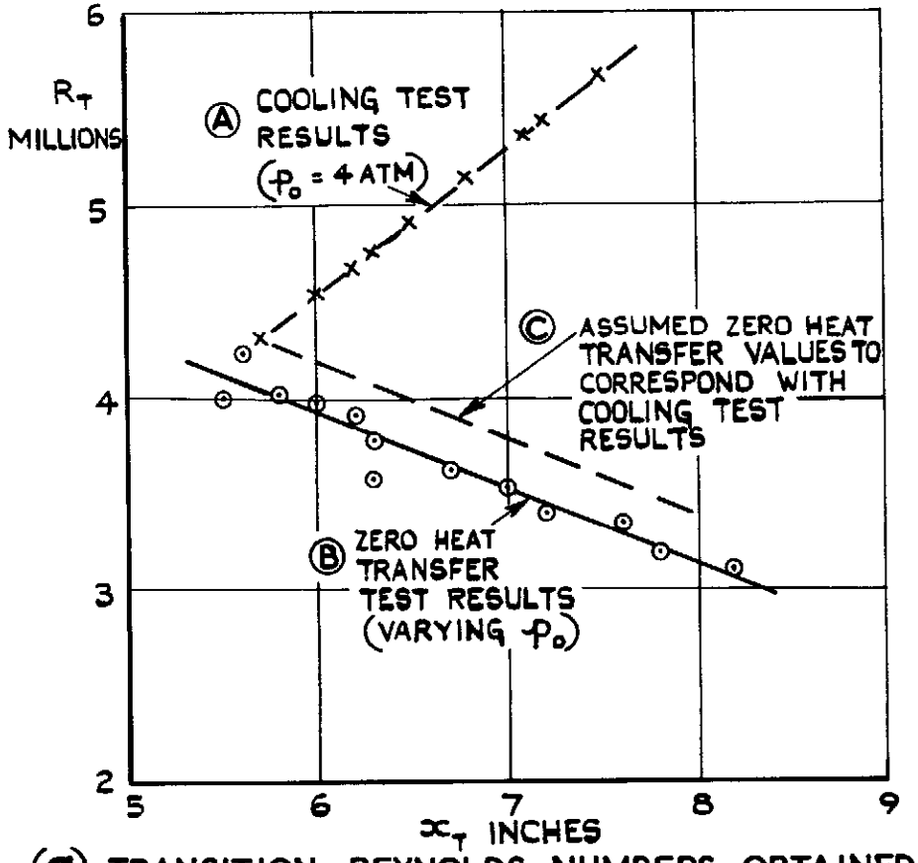

(a) TRANSITION REYNOLDS NUMBERS OBTAINED AT DIFFERENT DISTANCES FROM THE TIP (x_T).

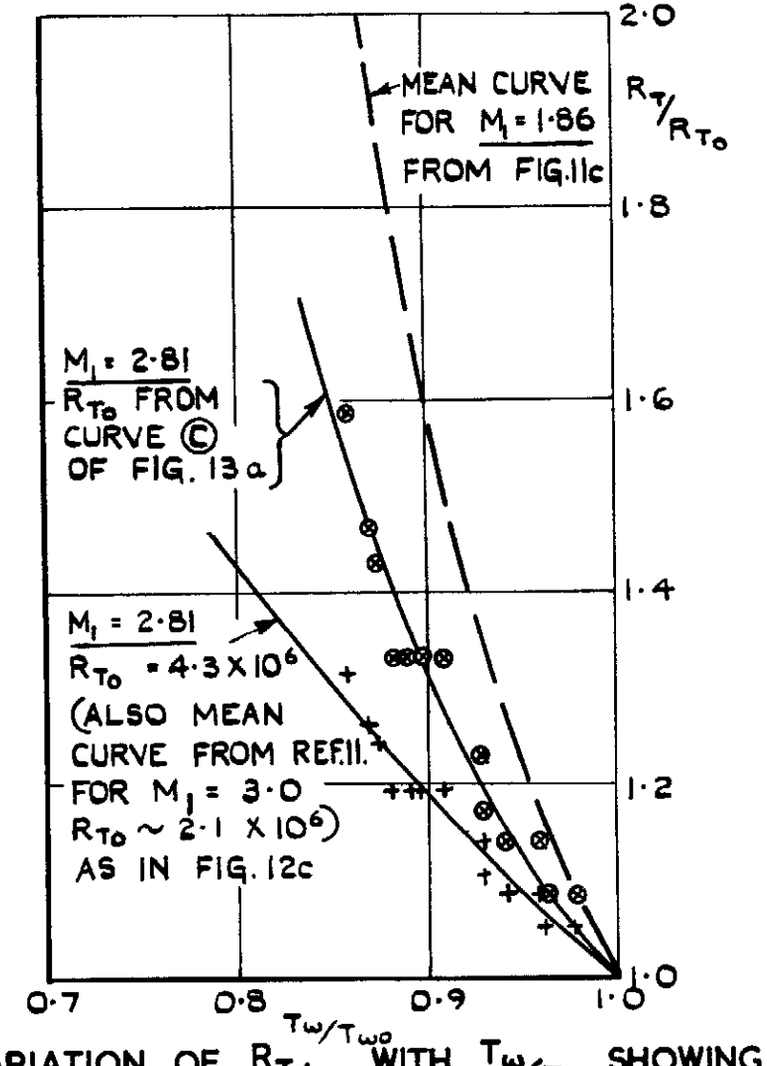

(b) VARIATION OF R_T/R_{To} WITH T_w/T_{wo} SHOWING EFFECT OF CHOICE OF R_{To}

FIG. 13. (a & b). ALTERNATIVE ANALYSIS OF TRANSITION RESULTS WITH COOLING AT M_∞ = 3·01 (M_1 = 2·81) (ZERO INCIDENCE).

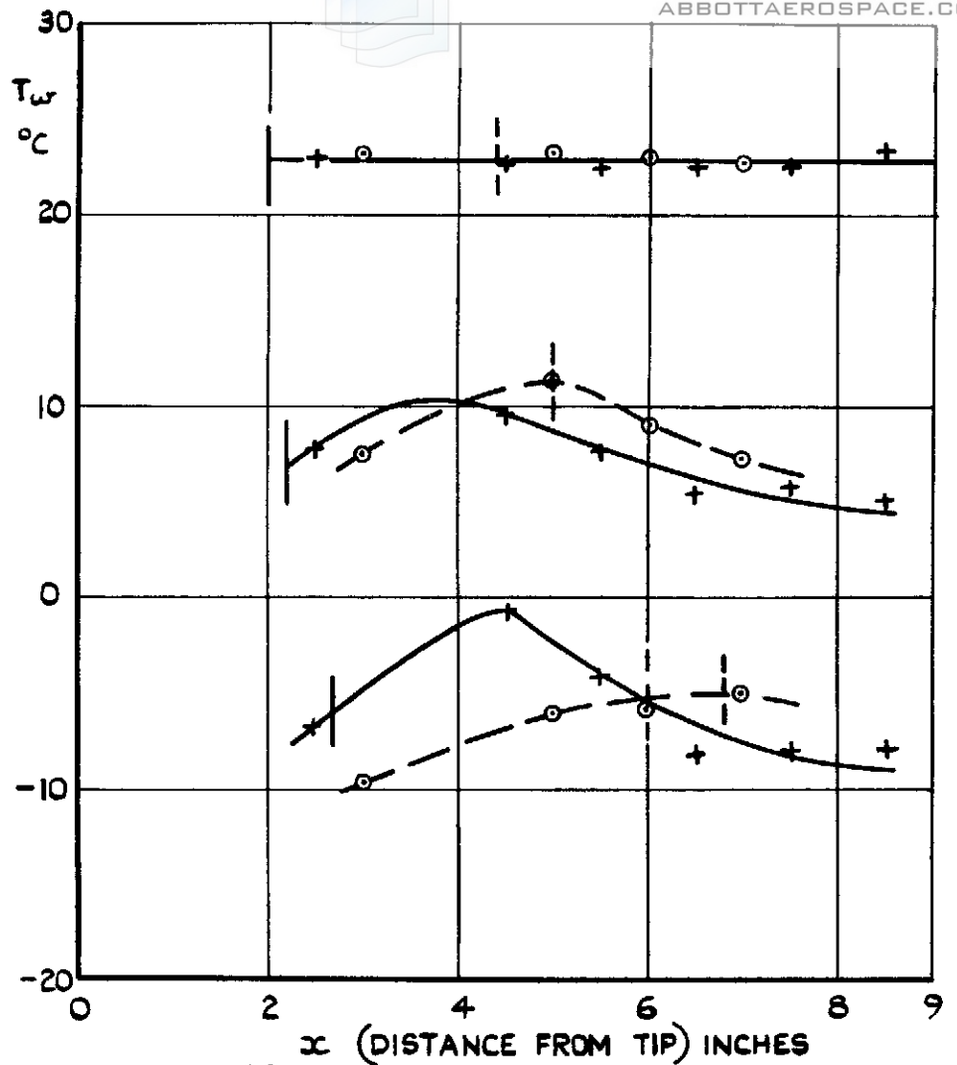

(a) $M_\infty = 1.97$ $P_0 = 3$ ATM.

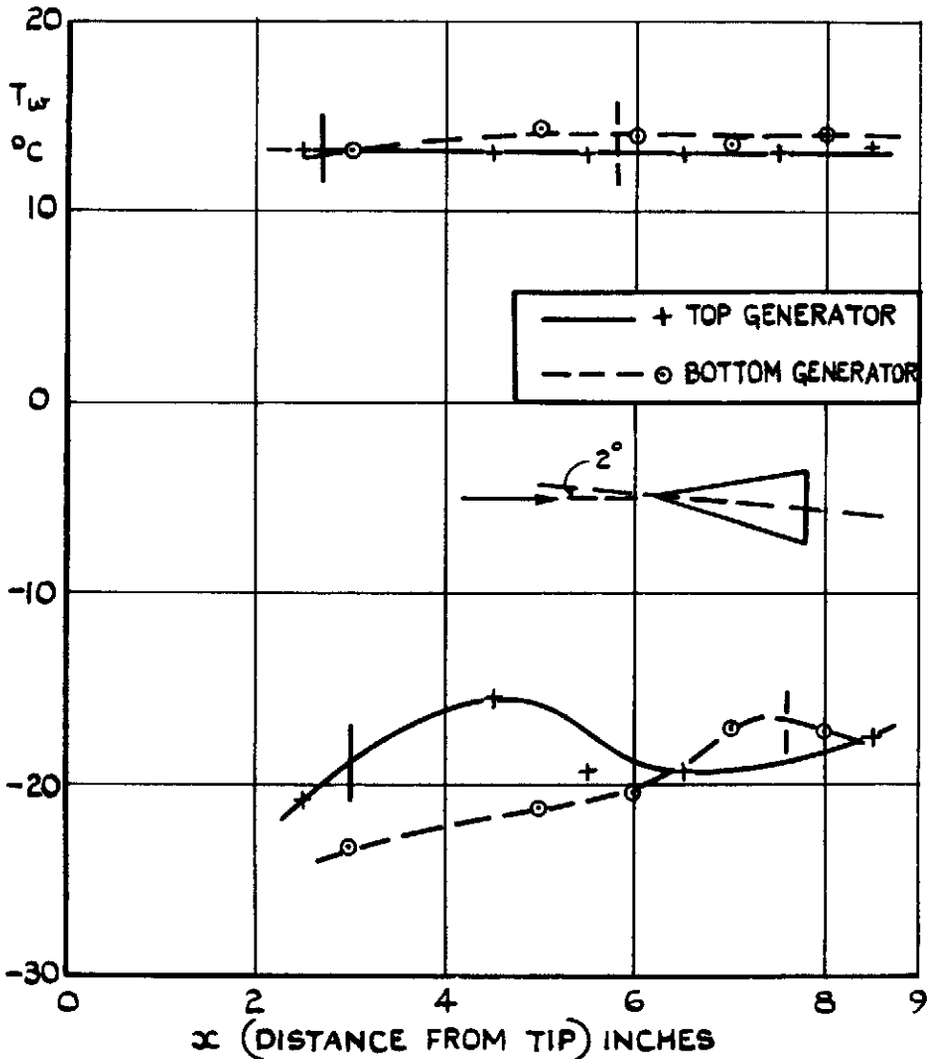

(b) $M_\infty = 3.01$ $P_0 = 4$ ATM.

FIG. 14. (a & b). DISTRIBUTIONS OF SURFACE TEMPERATURE ALONG THE 15° STEEL CONE AT +2° INCIDENCE
(COOLANT FLOWING FROM BASE TO TIP)

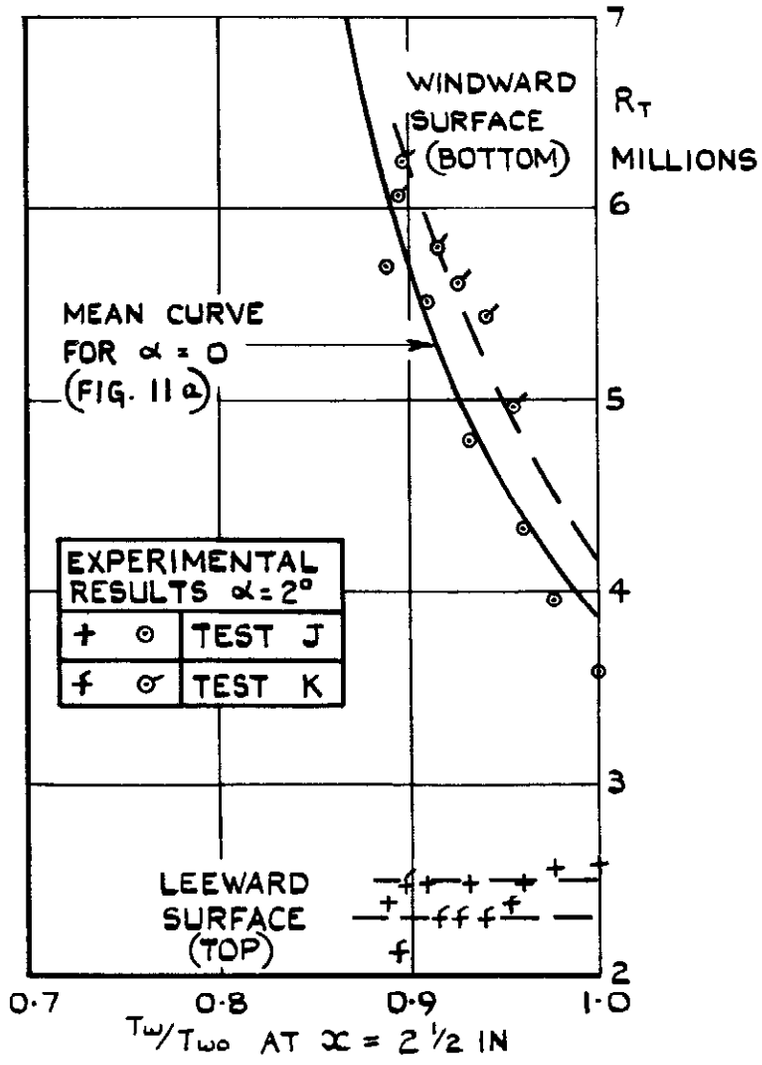

(a) $M_\infty = 1{\cdot}97$ $P_o = 3$ ATM (2 TESTS)

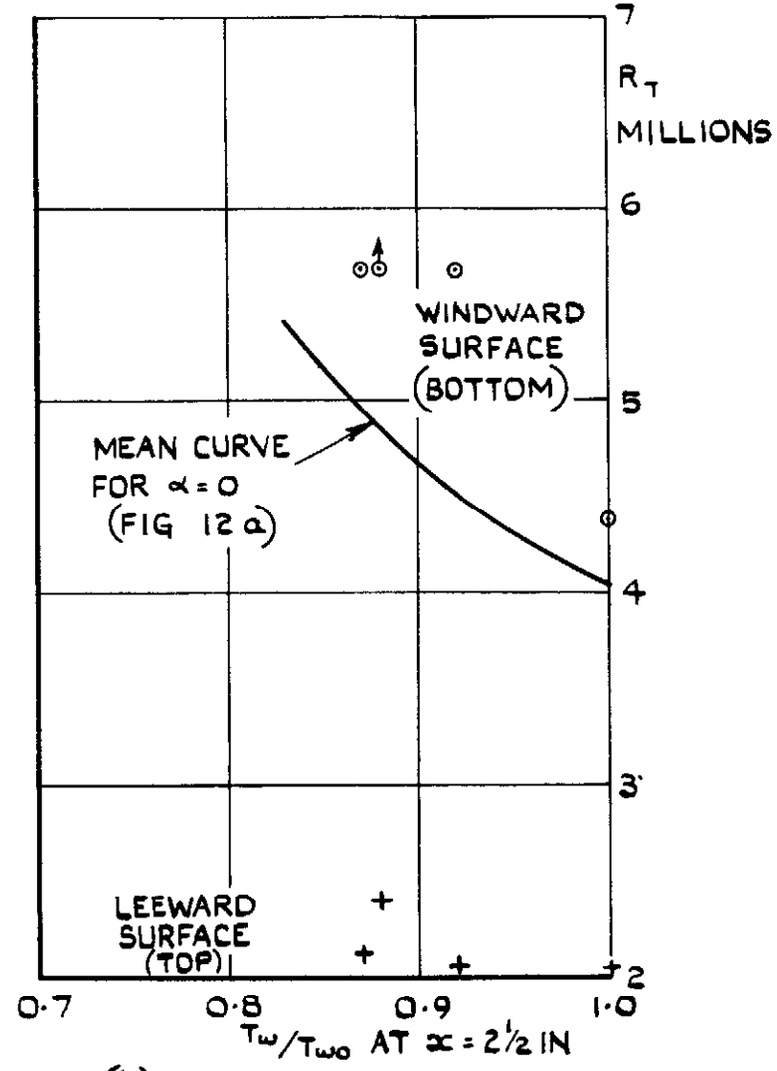

(b) $M_\infty = 3{\cdot}01$ $P_o = 4$ ATM

FIG.15.(a&b). EFFECT OF 2° POSITIVE INCIDENCE ON MOVEMENT WITH COOLING OF TRANSITION POINT ON 15° CONE.
(FROM SHADOWGRAPH)

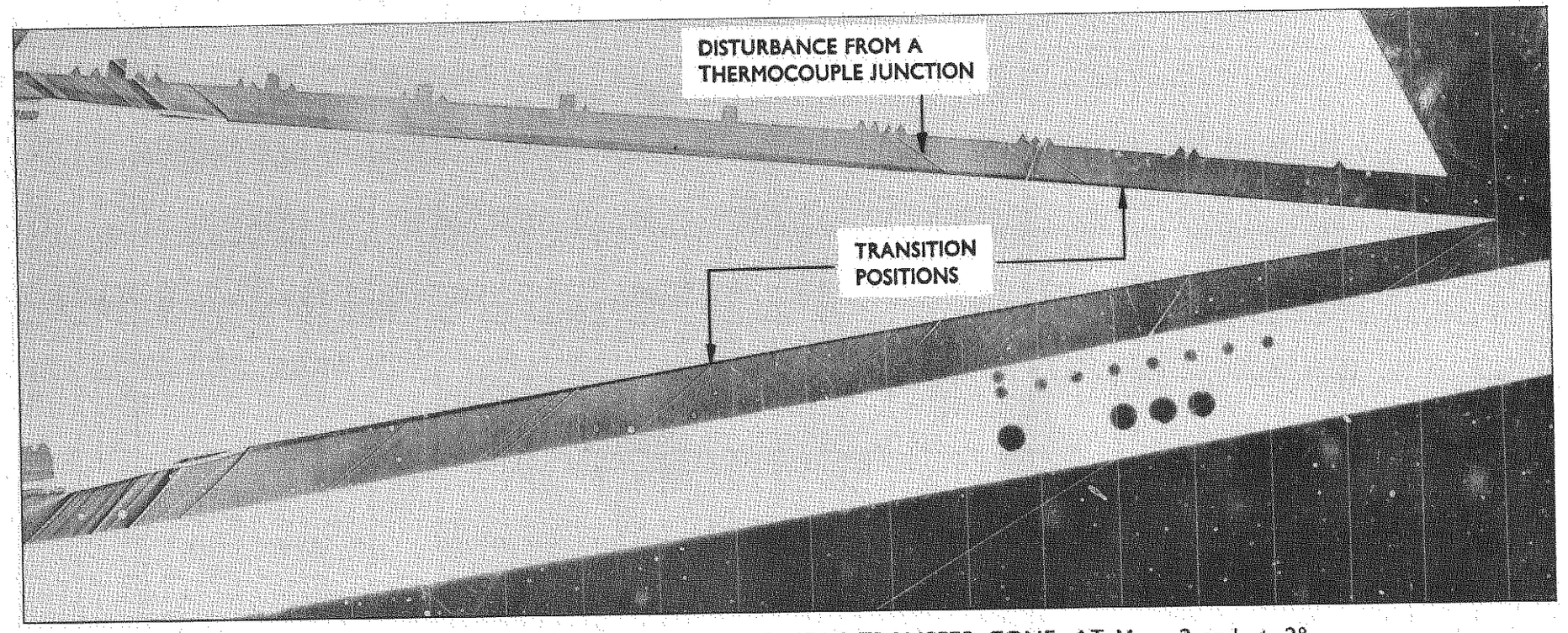

FIG.16. SHADOWGRAPH PICTURE OF THE HEAT TRANSFER CONE, AT M = 2 and + 2° INCIDENCE, ILLUSTRATING THE CHOSEN TRANSITION POSITIONS. (SOME DETAIL IS LOST IN PRINTING)

C.P. No. 381
(19,836)
A.R.C. Technical Report

Published by
HER MAJESTY'S STATIONERY OFFICE
To be purchased from
York House, Kingsway, London W C 2
423 Oxford Street, London W 1
13A Castle Street, Edinburgh 2
109 St. Mary Street, Cardiff
39 King Street, Manchester 2
Tower Lane, Bristol 1
2 Edmund Street, Birmingham 3
80 Chichester Street, Belfast
or through any bookseller

PRINTED IN GREAT BRITAIN

S.O. Code No. 23-9010-81

C.P. No. 381